ACS Chemical Neuroscience

pubs.acs.org/chemneuro

Research Article

Characterization of Homogeneous and Heterogeneous Amyloid-β42 Oligomer Preparations with Biochemical Methods and Infrared Spectroscopy Reveals a Correlation between Infrared Spectrum and Oligomer Size

Faraz Vosough and Andreas Barth*

Cite This: ACS Chem. Neurosci. 2021, 12, 473−488

Read Online

ACCESS | Metrics & More | Article Recommendations | Supporting Information

ABSTRACT: Soluble oligomers of the amyloid-β(1-42) (Aβ42) peptide, widely considered to be among the relevant neurotoxic species involved in Alzheimer's disease, were characterized with a combination of biochemical and biophysical methods. Homogeneous and stable Aβ42 oligomers were prepared by treating monomeric solutions of the peptide with detergents. The prepared oligomeric solutions were analyzed with blue native and sodium dodecyl sulfate polyacrylamide gel electrophoresis, as well as with infrared (IR) spectroscopy. The IR spectra indicated a well-defined β-sheet structure of the prepared oligomers. We also found a relationship between the size/molecular weight of the Aβ42 oligomers and their IR spectra: The position of the main amide I′ band of the peptide backbone correlated with oligomer size, with larger oligomers being associated with lower wavenumbers. This relationship explained the time-dependent band shift observed in time-resolved IR studies of Aβ42 aggregation in the absence of detergents, during which the oligomer size increased. In addition, the bandwidth of the main IR band in the amide I′ region was found to become narrower with time in our time-resolved aggregation experiments, indicating a more homogeneous absorption of the β-sheets of the oligomers after several hours of aggregation. This is predominantly due to the consumption of smaller oligomers in the aggregation process.

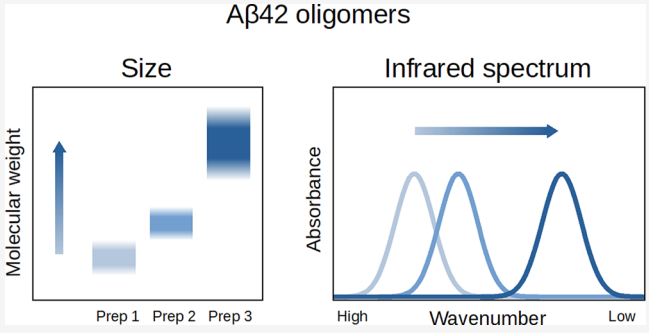

KEYWORDS: *Amyloid-β peptide, antiparallel β-sheet, FTIR spectroscopy, infrared spectroscopy, oligomer*

INTRODUCTION

Pathological changes or behavioral symptoms associated with Alzheimer's disease (AD) have been found to correlate with levels of soluble amyloid-β peptide (Aβ) in the brain or the cerebrospinal fluid.[1−4] As such, since about two decades ago, soluble oligomeric species have been mentioned as a major source of toxicity in AD, as well as in several other neurodegenerative diseases.[5] A number of Aβ oligomers with very different sizes and morphologies have been obtained from human/animal neural tissues or prepared *in vitro*, and their biological and neurotoxic activities were studied.[6−16] Many of these oligomers interfere with synaptic plasticity through inhibition of long-term potentiation in the hippocampus, a physiological process widely considered to be closely associated with learning and memory.[17,18] Of the several isoforms of Aβ, the 42-residue variant Aβ42 is considered to be pathologically relevant because of its neurotoxicity.[4]

A major difficulty in experimental studies of Aβ oligomers arises from their metastable and heterogeneous nature. *In vitro* preparations from monomeric Aβ solutions make it possible to control the oligomerization process in order to prepare stable and homogeneous Aβ oligomers. For this purpose, a number of protocols have been developed which mostly use detergents or fatty acids to stabilize oligomers of certain molecular weights and/or conformations.[19−22]

In 2005, Barghorn et al. reported the production of stable and homogeneous Aβ42 oligomers of different sizes via treatment of monomeric peptide solutions with low concentrations of sodium dodecyl sulfate (SDS). They prepared an Aβ42 oligomer of about 60 kDa, termed globulomer, which could inhibit long-term potentiation in hippocampal cell cultures and exhibited immune cross-reaction with Aβ42 aggregates from AD patients.[19] Similar findings were reported by Tew et al.[21] for Aβ40 and Aβ42, whose oligomer preparations were β-sheet rich and capable of impeding the

Received: October 7, 2020
Accepted: January 8, 2021
Published: January 18, 2021

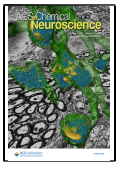

https://dx.doi.org/10.1021/acschemneuro.0c00642
ACS Chem. Neurosci. 2021, 12, 473−488

growth of cultured cortical neurons. To the contrary, Aβ peptides mostly adopt α-helical conformation at SDS concentrations above the critical micelle concentration.[23−26]

Recently Serra-Batiste et al.[22] produced detergent-stabilized Aβ42 oligomers within an environment of dodecyl phosphocholine (DPC) micelles. The prepared oligomer proved stable and was able to form pores in lipid bilayers.

Fourier transform infrared (FTIR) spectroscopy is a powerful experimental technique in studies of protein misfolding and aggregation.[27−34] This particularly stems from the sensitivity of the IR spectrum in the amide I region (around 1650 cm^{-1} or 6.1 μm) to the secondary structure of proteins and its potential to easily detect and distinguish β-sheets from other protein secondary structures. In addition, FTIR spectroscopy provides the possibility to study aqueous solutions with physiological buffers.

In the current study, detergent-induced oligomers of Aβ42 were produced and studied in D_2O solution. They were examined with blue native and denaturing gel electrophoresis to determine their size distribution. In addition, they were studied with FTIR spectroscopy to characterize and distinguish Aβ42 oligomers of different sizes and during the time course of aggregation. To the best of our knowledge, this work is among the first studies on FTIR spectral properties of defined-size Aβ oligomers. We establish a correlation between the IR spectrum and the size of the oligomers and show that the heterogeneity of the β-sheet structures varies with aggregation time. The results demonstrate the usefulness of FTIR spectroscopy for the analysis of β-sheet structures and establish new spectral markers for the structural interpretation of protein misfolding studies.

RESULTS AND DISCUSSION

Gel Electrophoretic Characterization of Detergent-Stabilized Aβ42 Oligomers. In order to prepare homogeneous Aβ42 oligomers of defined size, 100−120 μM monomeric peptide solutions of either synthetic or recombinant peptide (initially prepared at high pD) were incubated at two SDS concentrations (0.05 and 0.2%) in phosphate buffered saline (PBS) buffer, pD 7.4, as well as at 5.5 mM DPC in Tris-HCl buffer (pD 9). All solutions were incubated at 37 °C for 24 h.

Making use of detergents, most notably SDS, is known to be crucial for stabilization of Aβ oligomers of certain sizes and therefore for obtaining homogeneous Aβ oligomer solutions.[19−21] This also has consequences for the analysis of SDS-polyacrylamide gel electrophoresis (SDS-PAGE) results, which are not readily interpretable when used on their own. High concentrations of SDS (1 or 2%) in SDS-PAGE sample buffers are found to both induce oligomerization of the Aβ peptides and decompose large oligomers.[35,36] Chemical cross-linking methods can be used to overcome this obstacle;[37] however, recent studies have revealed that even when combined with cross-linking methods, SDS-PAGE may be misleading in size estimation of Aβ oligomers.[38] Therefore, we opted to use Blue Native-PAGE (BN-PAGE) alongside SDS-PAGE to characterize the prepared oligomeric samples. BN-PAGE has been employed successfully in studies of Aβ-containing samples from *in vitro* and *in vivo* sources.[39,40]

The BN-PAGE results are shown in Figures 1 and 2. Figure 1 presents the results for oligomers formed at two different concentrations of SDS. In addition, oligomers formed under the same conditions (buffer solution, pD, incubation time and temperature) but without SDS are analyzed on the gel. Distinct bands are resolved when SDS is present (lanes 2−5 and 7 and 8). To the contrary, oligomers formed in the absence of SDS produce faint smears on the blue native gel (lanes 6 and 9), although the same amount of the peptide was loaded. This observation confirms the role of the detergent SDS in stabilizing certain Aβ42 oligomers.[19−21] In addition, bands corresponding to different oligomer sizes are observed for the peptide incubated at different SDS concentrations. The lower SDS concentration (0.05%) produces larger oligomers (the band extends from approximately 30−45 kDa), while the higher concentration (0.2%) gives rise to smaller oligomeric structures (approximately 4−16 kDa).

It is also interesting to compare the prepared oligomers formed from synthetic and recombinant Aβ42 peptides. Both types of the peptide produce oligomers of the same two sizes, depending on the SDS concentration. The bands for the oligomers from the recombinant source (Figure 1, lanes 7−8), however, are not as sharp and intense as those obtained for the

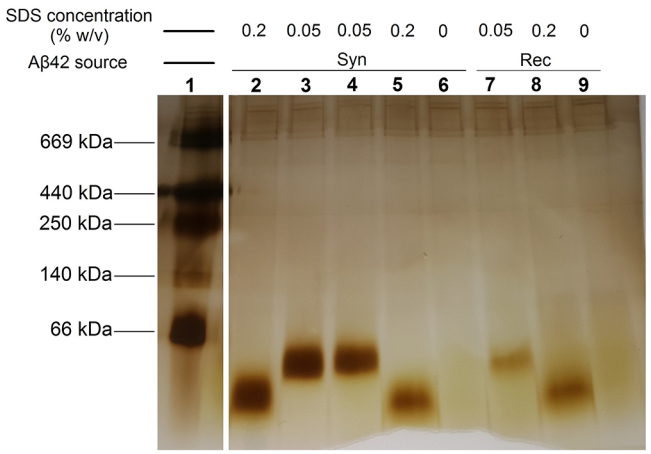

Figure 1. BN-PAGE analysis of oligomers of synthetic and recombinant Aβ42 in presence and absence of SDS. Lane 1 = standard protein ladder; Lane 2, 5 = synthetic peptide, 0.2% SDS; Lanes 3, 4 = synthetic peptide, 0.05% SDS; Lane 6 = synthetic peptide in PBS, no detergent; Lane 7 = recombinant peptide, 0.05% SDS; Lane 8 = recombinant peptide, 0.2% SDS; Lane 9 = recombinant peptide in PBS, no detergent. All samples were incubated for 24 h.

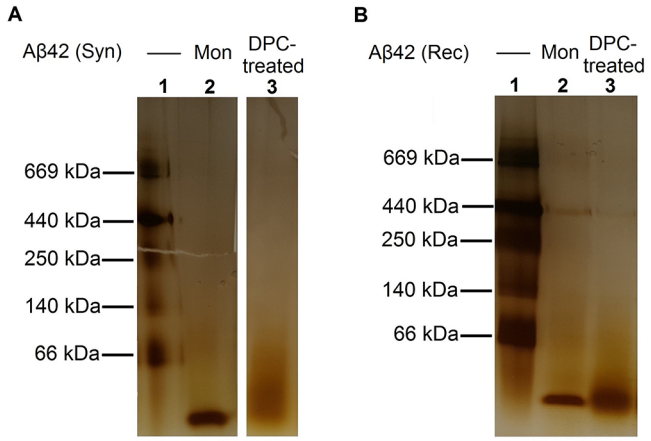

Figure 2. BN-PAGE analysis of the DPC-stabilized Aβ42 oligomers for (A) synthetic peptide and (B) recombinant peptide. Lane 1 = standard protein ladder; Lane 2 = monomeric Aβ42; Lane 3 = DPC-stabilized oligomers. All samples were incubated for 24 h.

https://dx.doi.org/10.1021/acschemneuro.0c00642
ACS Chem. Neurosci. 2021, 12, 473−488

synthetic Aβ42 peptide (Figure 1, lanes 2−5), although the same amount of peptide was loaded. This difference was observed in repeated experiments and indicates that the oligomer preparations with the recombinant peptide are more heterogeneous than those with the synthetic peptide. Nevertheless, our observation of relatively homogeneous Aβ42 oligomers at low SDS concentrations is in contrast to other oligomeric solutions of Aβ42, including the oligomers prepared *in vitro* in F12 medium, which were characterized as heterogeneous when investigated by both SDS-denaturing and BN gel electrophoresis.[9,39]

As shown in Figure 2, DPC treatment produces oligomers which appear as broadened bands or smears on the blue native gel (panels A and B, lane 3). The broadened band resolves in the low molecular weight regions, extending from the monomeric band toward larger sizes, mostly under the 66 kDa mark. Therefore, oligomeric solutions of Aβ42 formed in the presence of DPC are less homogeneous compared to SDS-stabilized oligomers for the same peptide under the conditions used in this study. In this case, the preparation with the recombinant peptide seems to be somewhat more homogeneous as its band is more dense in the low molecular weight range that is close to the monomer band.

Although BN-PAGE is helpful in the analysis and characterization of actual oligomeric species from solutions of aggregating peptides and proteins, it only provides rough estimations of the protein sizes, due to the method's limited resolving capacity. In order to gain more information about the size distribution of the prepared Aβ42 oligomers and to make it possible to compare the results with other published works,[19,22] the oligomer samples were also studied with higher resolution denaturing SDS-PAGE, which provides a better size resolution. We used two SDS-PAGE systems, Tris-glycine (Laemmli) and Tris-Tricine, so that both large and small size oligomers were resolved and observed.

Figure 3 shows the Tris-glycine SDS-PAGE results for oligomers stabilized by either SDS or DPC. Figure 4 shows the

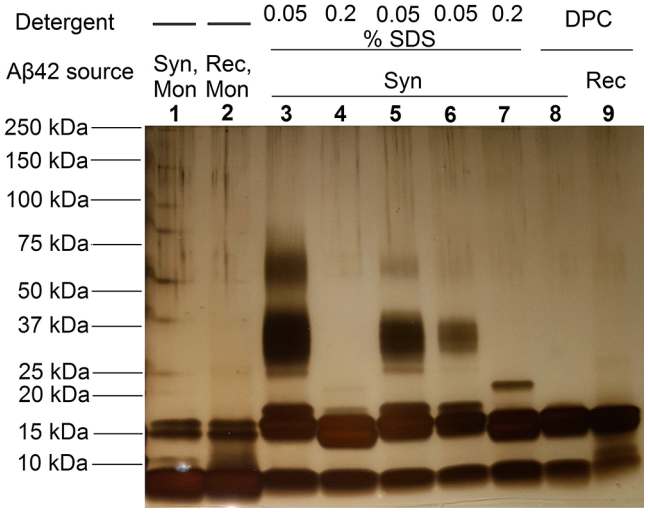

Figure 3. Tris-glycine SDS-PAGE analysis of SDS and DPC-stabilized Aβ42 oligomers. Lane 1 = monomeric synthetic Aβ42; Lane 2 = monomeric recombinant Aβ42; Lanes 3, 5, 6 = 0.05% SDS treated in synthetic Aβ42; Lanes 4, 7 = 0.2% SDS treated in synthetic Aβ42; Lane 8 = DPC treated synthetic Aβ42; Lane 9 = DPC treated recombinant Aβ42. All samples were incubated for 24 h.

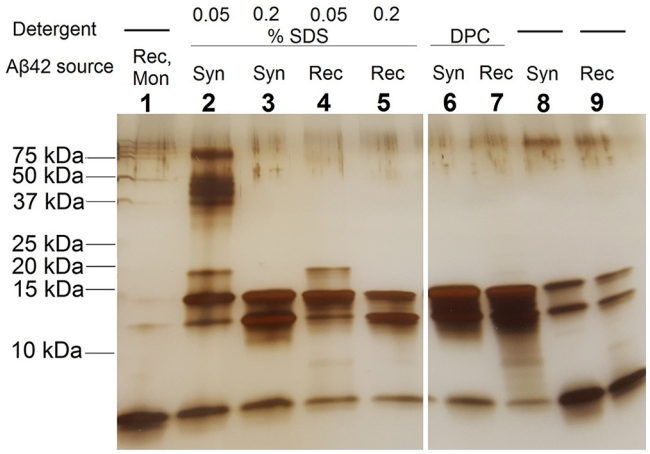

Figure 4. Tris-Tricine SDS-PAGE analysis of SDS-stabilized, DPC-stabilized, and detergent-free Aβ42 oligomers. Lane 1 = monomeric recombinant Aβ42; Lane 2 = 0.05% SDS treated synthetic peptide; Lane 3 = 0.2% SDS treated synthetic peptide; Lane 4 = 0.05% SDS treated recombinant peptide; Lane 5 = 0.2% SDS treated recombinant peptide; Lane 6 = DPC-stabilized synthetic peptide; Lane 7 = DPC-stabilized recombinant peptide; Lane 8 = synthetic peptide in PBS, no detergent; Lane 9 = recombinant peptide in PBS, no detergent. All samples were incubated for 24 h.

respective results on a Tris-Tricine gel, used to resolve lower molecular weight species. Monomeric solutions produce an intense band below 10 kDa on the Tris-glycine gel (Figure 3, lanes 1−2), as well as a double band around 15 kDa, which could be attributed to trimers and tetramers of the peptide. In contrast, this double band is very weak on the Tris-Tricine gel (Figure 4, lane 1), and the same solutions always generate single bands on BN-PAGE gels (Figure 2A,B, lane 2). Our observed pattern of monomeric, trimeric, and tetrameric bands even for monomeric Aβ42 solutions is in line with many previous reports.[19,35,41] Formation of oligomers on the SDS-PAGE gel could be an artifact due to the effect of SDS in the sample buffer.[35] In line with this assumption, the oligomer bands seem to be stronger on the Tris-glycine gel with 2% SDS in the sample buffer than on the Tris-Tricine gel with 1% SDS. Moreover, spectroscopic methods (IR absorption and CD) confirm the expected random coil structure for the peptide in these solutions (see below for a description of the IR results).

The SDS-PAGE separation profiles for Aβ42 in 0.2% SDS are shown in lanes 4 and 7 of Figure 3 and lanes 3 and 5 of Figure 4. Compared to monomeric solutions, the band below 10 kDa has a lower intensity, whereas the trimer and tetramer bands have a higher intensity. Additionally, a band near 20 kDa is seen on the Tris-glycine gel with different intensities in the two experiments (Figure 3, lanes 4 and 7). Its absence for the monomeric samples shown in lanes 1 and 2 of the gel confirms that it was not generated from monomers by the higher SDS concentration in the SDS-PAGE sample buffer than in the original sample. The 15−20 kDa molecular weight range for the largest oligomers seen by SDS-PAGE is in agreement with the upper size limit from BN-PAGE of the same samples.

In lanes 3, 5, and 6 of Figure 3, results of three independent repeats for the synthetic Aβ42 peptide in 0.05% SDS for the Tris-glycine gel are presented. Bands below 10 kDa corresponding to monomeric or dimeric peptides are still present, but they are less intense than for the monomeric peptide, which suggests that monomers or dimers have been

https://dx.doi.org/10.1021/acschemneuro.0c00642
ACS Chem. Neurosci. 2021, 12, 473−488

consumed to produce larger oligomers of the peptide. In BN-PAGE experiments of 0.05% SDS-stabilized samples (Figure 1), no band corresponding to monomers is observed. Therefore, the presence of the monomeric band in SDS denaturing gel could be indicative of a partial decomposition of the formed oligomers in the SDS-PAGE sample buffer. Instead of double bands observed for monomeric solutions near 15 kDa, triple or thicker bands are observed in the case of the 0.05% SDS-stabilized samples. In addition, an intense smear is observed between 25 and 37 kDa, as well as a band at approximately 60 kDa with different intensities for independent repeats on the Tris-glycine gel (Figure 3, lanes 3, 5, and 6). The dominant band is the one at around 37 kDa, while the 60 kDa band has variable intensity in the experiments shown and is completely absent in several repeat experiments (data not shown).

The highest molecular weight detected on the Tris-glycine gel (around 60 kDa) is close but somewhat larger than the upper size limit for the same oligomeric samples on the BN-PAGE gel (Figure 1, lanes 3 and 4), whereas the species near 30 kDa in SDS-PAGE are close to the lower size limit seen in BN-PAGE. Species smaller than approximately 30 kDa are not seen in BN-PAGE but in both types of SDS-PAGE gels, likely because they were induced by the 1 or 2% SDS concentration in the SDS-PAGE sample buffer. Therefore, they seem to be the products of decomposition of the prepared oligomer. In line with this assumption, the repeats for the small and large SDS-stabilized oligomers produce partially different separation patterns on the Tris-glycine SDS-PAGE gel (Figure 3), possibly because of different incubation times at 2% SDS before loading on the gel; meanwhile, the same samples give rise to similar bands in the BN-PAGE analysis (Figure 1).

Very similar results for synthetic Aβ in 0.05% SDS were obtained for the Tris-glycine and Tris-Tricine gel, but the respective bands resolve at somewhat higher molecular weights on the latter (Figure 4, lane 2). In contrast, the higher molecular weight species are not observed for the recombinant peptide on the Tris-Tricine gel (Figure 4, lane 4) under the same incubation conditions, although the band positions of the oligomers from synthetic and recombinant are similar in BN-PAGE. It appears that the oligomers of the recombinant Aβ42 are less resistant to the high SDS concentrations, compared to the corresponding oligomers from the synthetic peptide.

The overall separation profile on SDS-PAGE gels for our globulomers of synthetic Aβ42 is in agreement with the results from the SDS-PAGE analysis in the original report of globulomer preparation, where a maximum molecular weight of around 50 kDa was reported for globulomers.[19] We conclude that we have obtained the same oligomers as in the original publication,[19] while different analysis methods obtain different values for their molecular weights. This was also observed by Barghorn et al. when they compared gel electrophoresis results with those from size exclusion chromatography. Probably the best estimate for the molecular weight of the larger SDS-Aβ42 oligomer is their value of about 60 kDa from size exclusion chromatography of cross-linked oligomers. This is close to the higher molecular weight limit in our BN-PAGE experiments (Figure 1) and corresponds to the highest molecular weight band on our Tris-glycine SDS-PAGE gels (Figure 3, 60 kDa corresponding approximately to dodecamers). Then, the size of the small SDS-Aβ42 oligomers is also likely to be larger than indicated by their average band position obtained by BN PAGE. The higher molecular weight limit of this band is around 20 kDa, which corresponds to tetramers.

DPC-stabilized Aβ42 oligomers produce separation patterns similar to the monomeric peptide on the Tris-glycine (Figure 3, lanes 8 and 9) and the Tris-Tricine (Figure 4, lanes 6 and 7) gels, but the monomeric band intensity is reduced and the trimer-tetramer bands are more intense for the oligomer preparations, which agrees with Serra-Batiste et al.[22] In a recent study, making use of ion mobility-mass spectrometry, the Aβ42 oligomeric solution formed in the presence of DPC was characterized as containing small oligomers up to hexamers.[42]

While the methods for homogeneous oligomer preparation in this study were based on earlier work,[19,22] they were modified here so as to be compatible with the protocol developed in our laboratory for the preparation of monomeric Aβ solutions and with the requirements for IR spectroscopy. Though it is possible that the peptide behaves differently in the used D_2O medium than in the H_2O medium of the original protocols, the gel electrophoresis results show that oligomers of the same molecular weights were prepared in our study as in the original reports.[19,22] We were able to produce the SDS-stabilized small size oligomers at a 4-fold lower concentration of the peptide than reported by Barghorn et al.[19] They reported the smaller oligomers as intermediates in the pathway leading to the formation of the larger globulomers and prepared the latter by dilution of the small oligomer preparation. However, in our experiments, the two different oligomers were produced independently and directly at the same peptide concentration (100 μM), just after being exposed to different concentrations of SDS. This shows that the dedicated preparation of the smaller oligomers is not necessary to produce the globulomers. Our large oligomers were already formed after 6 h of incubation at 0.05% SDS concentration, with no traces of small oligomers on the BN-PAGE gel (data not shown). At this time point, the SDS concentration is reduced from 0.2 to 0.05% in the original protocol.[19]

Most of the studies on *in vitro* prepared oligomeric Aβ species, including those on the detergent-stabilized oligomers used here, have been conducted using peptides of synthetic origin.[19−22,39] However, it is known that synthetic and recombinant Aβ42 peptides behave differently in terms of both aggregation tendency and biological activity. Recombinant Aβ42 aggregates faster and is neurotoxic at lower concentrations, in comparison to its synthetic counterpart.[43,44] Therefore, it is also relevant to study the recombinant peptide, and we have used Aβ42 peptides from both sources. The recombinant Aβ42 proved more difficult to form SDS-stabilized globulomers, and the prepared globulomeric structures were more sensitive to the high SDS concentrations used in SDS gel electrophoresis than those formed with the synthetic peptide. In contrast, the DPC-stabilized oligomers seemed to be more homogeneous for the recombinant peptide.

SDS-PAGE and Western Blot Analysis of Detergent-Free Aβ42 Oligomers. In addition to detergent-stabilized oligomers, we also prepared samples without detergent. Some of them were incubated for 24 h in low-binding reaction tubes in order to compare them to the preparations with the detergent. Others were used for the time-resolved experiments, which lasted up to 18 h.

Separation profiles of oligomers in neutral-pD PBS buffer in the absence of any detergents are shown in lanes 8 and 9 of Figure 4. Bands for monomers, trimers, and tetramers were

https://dx.doi.org/10.1021/acschemneuro.0c00642
ACS Chem. Neurosci. 2021, 12, 473−488

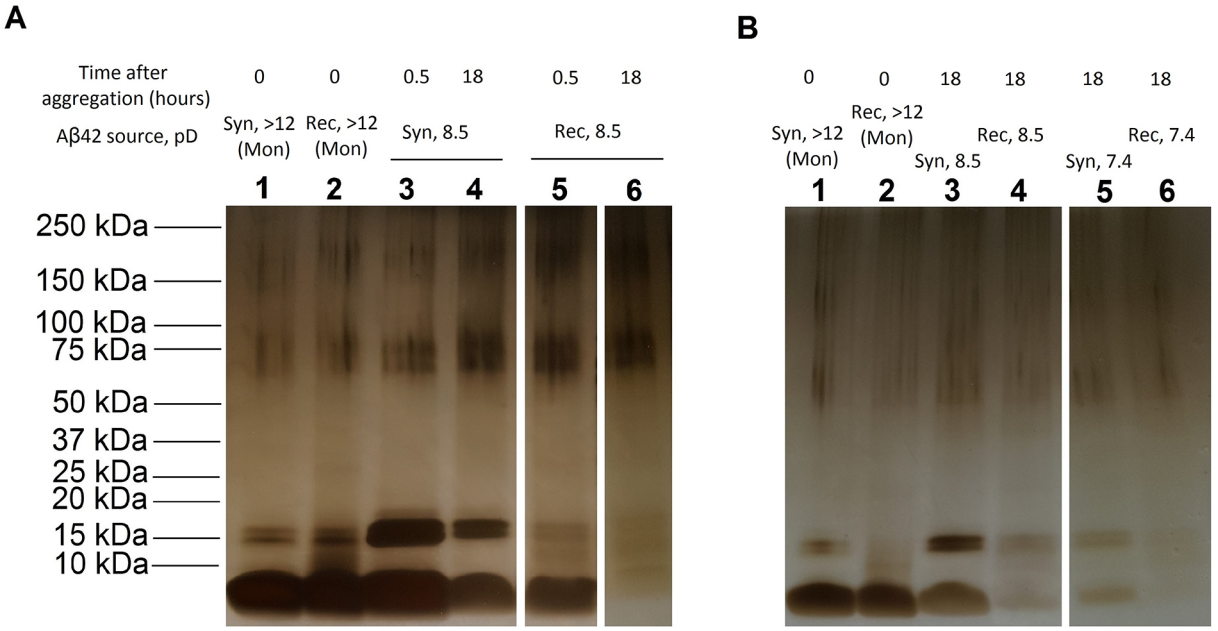

Figure 5. Tris-glycine SDS-PAGE analysis of detergent-free Aβ42 preparations. The Aβ42 monomers are compared to oligomers formed inside the IR cuvette in kinetic experiments. (A) The results from two time-points at pD 8.5 are shown. Lane 1 = monomeric synthetic peptide; Lane 2 = monomeric recombinant peptide; Lane 3 = oligomers of the synthetic peptide after 30 min at pD 8.5; Lane 4 = oligomers of the synthetic peptide after 18 h at pD 8.5; Lane 5 = oligomers of the recombinant peptide after 30 min at pD 8.5; Lane 6 = oligomers of the recombinant peptide after 18 h at pD 8.5. (B) The results for long-term incubation at two pD values are shown. Lane 1 = monomeric synthetic peptide; Lane 2 = monomeric recombinant peptide; Lane 3 = oligomers of the synthetic peptide after 18 h at pD 8.5; Lane 4 = oligomers of the recombinant peptide after 18 h at pD 8.5; Lane 5 = oligomers of the synthetic peptide after 18 h at pD 7.4; Lane 6 = oligomers of the recombinant peptide after 18 h at pD 7.4.

observed, as well as bands of much larger molecular weights on the top of the gel. However, it is not possible to estimate the molecular weights of such species on a Tris-Tricine gel.

Tris-glycine SDS-PAGE results of samples after almost 18 h of incubation in the IR cuvette during the time-resolved experiments are shown in Figure 5 and compared to the alkaline (pD 12.4−12.7), monomeric solutions (lanes 1 and 2 in panels A and B). Panel A shows the results for different time points at pD 8.5. Lanes 3 and 5 show the results after 30 min of incubation, and lanes 4 and 6 display the results after at least 18 h. At the early time point (lanes 3 and 5), monomers and small oligomers are prominent for both the synthetic and the recombinant peptide, but after almost 18 h (lanes 4 and 6), their concentration is significantly decreased. Bands for higher molecular weight species (60−250 kDa) appear to be stronger for the oligomer preparations than for the monomer preparations. However, these differences are less clear-cut than those for small oligomers and monomers. The size distribution for the recombinant peptide after almost 1 week was also studied and found to be similar to the 18 h incubated sample (data not shown). The effect of long-term (18 h) incubation at two different pD values is shown in panel B. The concentrations of monomers and small oligomers are even lower after 18 h of incubation at pD 7.4 (lanes 5 and 6) than at pD 8.5 (lanes 3 and 4). Under all conditions, the low molecular weight bands are stronger for the synthetic peptide than for the recombinant peptide. These results demonstrate the higher aggregation propensity of recombinant Aβ42, which is consistent with previous studies.[43,44]

Because large oligomers were difficult to detect on the SDS-PAGE gel, the Western blot assay with the anti-β-amyloid antibody 6E10 was used after SDS-PAGE on Tris-glycine gels. The results are shown in Figure 6. As observed, heterogeneous

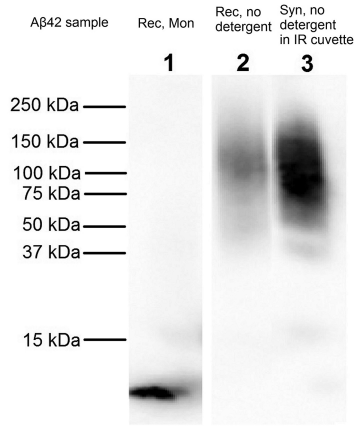

Figure 6. Western blot analysis of SDS-stabilized and detergent-free Aβ42 preparations separated with SDS-PAGE on Tris-glycine gels. Samples, except for the one in lane 3, were prepared from the recombinant peptide. Lane 1 = monomeric Aβ42; Lane 2 = oligomers formed in detergent-free phosphate buffer inside the IR cuvettes after 18 h at pD 8.5; Lane 3 = oligomers of the synthetic peptide formed in PBS (pD 7.4) in absence of detergent after 24 h of aggregation in low-binding reaction tubes.

Aβ42 oligomers formed in absence of detergent are resistant to high SDS concentrations (2% SDS, as in the SDS-PAGE sample buffer) and appear largely as a smear between 50 and 250 kDa on the blot (lanes 2 and 3 for recombinant and synthetic peptide, respectively), which is similar to the molecular weight range in which a smear is observed with SDS-PAGE (Figure 5).

Secondary Structure of Detergent-Stabilized Aβ42 Oligomers. Our oligomer preparations were also studied by transmission FTIR spectroscopy in aqueous (D_2O) solution, in

https://dx.doi.org/10.1021/acschemneuro.0c00642
ACS Chem. Neurosci. 2021, 12, 473−488

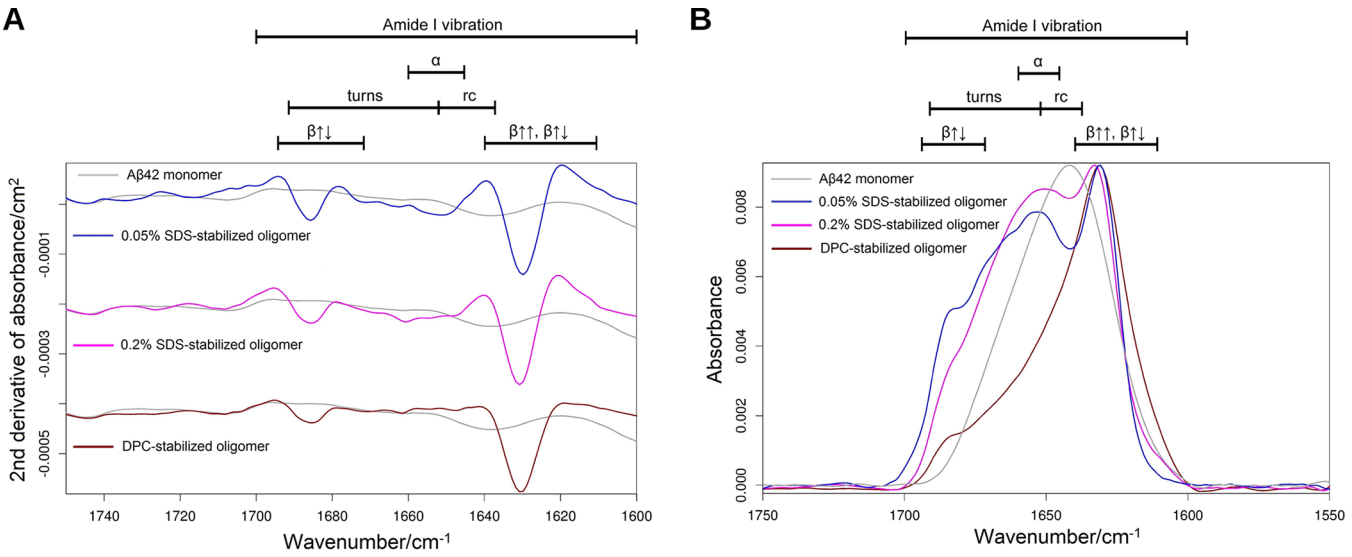

Figure 7. (A) Second derivatives of IR absorbance spectra for monomeric synthetic Aβ42, as well as detergent-stabilized oligomers of the same peptide after 24 h of incubation in low-binding reaction tubes. Gray = monomeric Aβ42; blue = 0.05% SDS-stabilized oligomers; purple = 0.2% SDS-stabilized oligomers; brown = DPC-stabilized oligomers. The monomer spectrum is the same in all cases. Spectra are shown for individual experiments. The middle and bottom oligomer spectrum are normalized to the intensity of the main band in the top spectrum. The maximum intensity values of the main band in the original spectra were as follows: purple (0.2% SDS-stabilized oligomers) = −0.00014 cm^2; brown (DPC-stabilized oligomers) = −0.00017 cm^2. (B) Absorbance spectra after buffer subtraction, baseline correction, and normalization in relation to the 0.05% SDS-stabilized oligomers. The color codes are the same as in panel A. The maximum absorbance values for normalized spectra were as follows: gray (monomeric Aβ42) = 0.008; purple (0.2% SDS-stabilized oligomers) = 0.013; brown (DPC-stabilized oligomers) = 0.017. Approximate spectral ranges for different secondary structures are indicated on the top of each panel using the following abbreviations: α = α-helix, $\beta\uparrow\uparrow$ = parallel β-sheet, $\beta\uparrow\downarrow$ = antiparallel β-sheet, rc = random coil.

a different mode from many other reports, which have utilized the attenuated total reflection (ATR) mode of IR spectroscopy with dried samples. We used aqueous samples, because solvent evaporation may modify Aβ aggregates. Accordingly, we have observed formation of β-sheet structures from monomeric alkaline solutions of unstructured Aβ42 upon solvent evaporation on an ATR crystal (data not shown). The use of aqueous solution also made it possible to perform kinetic measurements, providing insight into the structure and dynamics of these metastable and polydisperse aggregates.

Typical IR spectra for the detergent-induced oligomers obtained with the synthetic peptide, as well as for the starting monomeric solution, are shown in Figure 7. The spectra in panel A are the second derivatives of the absorbance in the amide I′ region (the prime indicates the amide I vibration of deuterated amide I′ groups). In second derivative spectra, component bands of the absorbance spectra appear as negative bands. Respective absorbance spectra are shown in panel B of Figure 7.

In case of the monomeric Aβ42 solutions, the peptide backbone band in the amide I′ region is found around 1639–1640 cm^{-1}, indicating random coil conformation in agreement with the mostly monomeric state observed in the BN-PAGE experiments. Spectra for SDS- and DPC-stabilized Aβ42 oligomers are also shown in Figure 7. Their main band is found at approximately 1630 cm^{-1}, which is 10 cm^{-1} lower than the random coil band of monomeric Aβ. It also appears larger and much sharper in the second derivative spectra of Figure 7A. This β-sheet band position is lower than the position of approximately 1635 cm^{-1} found for 2- and 3-stranded sheet models.[45−47] In addition, the splitting between high and low wavenumber bands is larger for our oligomers (approximately 56 cm^{-1}) than for the β-sheet models

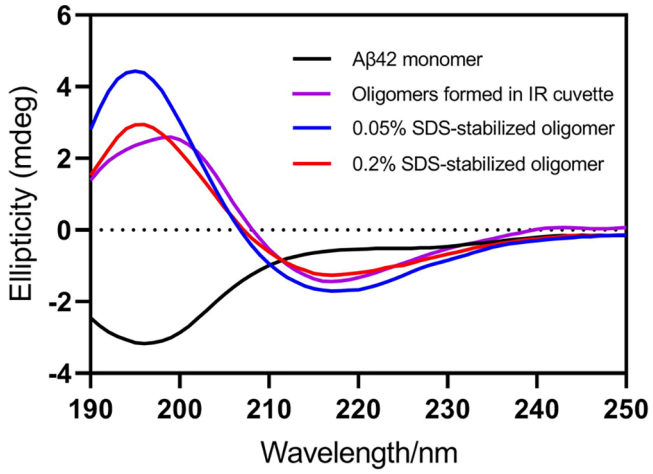

Figure 8. Circular dichroism spectra of synthetic Aβ42 peptide oligomers. Blue and red = homogeneous oligomers at SDS concentrations of 0.05% (blue) and 0.2% (red) after 24 h of incubation. Violet = oligomeric solution inside the IR cuvette in phosphate buffer, no detergent at pD 7.4 after 18 h of aggregation. Black = monomeric Aβ42.

(approximately 40 cm^{-1}). We conclude therefore that the number of strands in the β-sheets of our oligomers is larger than three. An empirical correlation predicts around 10 strands for a β-sheet maximum at 1630 cm^{-1}.[48]

In addition to the main band near 1630 cm^{-1}, a smaller band at higher wavenumbers is also observed near 1685 cm^{-1}. Such a double-band feature in the amide I region of IR spectra for protein oligomers and early aggregates has been repeatedly reported and is consistent with the accepted IR signature for antiparallel β-sheets,[29,49−51] which is in line with theoretical

https://dx.doi.org/10.1021/acschemneuro.0c00642
ACS Chem. Neurosci. 2021, 12, 473−488

Table 1. IR Band Positions and Bandwidths for Aβ42 Oligomers[a]

Aβ42 sample (n = number of experiments)	incubation time (h)	width at half height for low wavenumber component (cm^{-1})	position of low wavenumber component (cm^{-1})	position of high wavenumber component (cm^{-1})
0.05% SDS, synthetic (n = 3)	24	7.3 ± 0.1	1629.6 ± 0.4	1686.1 ± 0.2
0.05% SDS, recombinant (n = 3)	24	8.0 ± 0.8	1629.1 ± 0.5	1686.5 ± 0.9
0.05% SDS, recombinant (n = 1)	120	10.7	1626.8	1685.8
0.2% SDS, synthetic (n = 2)	24	7.0 ± 0.2	1630.4 ± 0.5	1685.7 ± 0.3
0.2% SDS, recombinant (n = 2)	24	7.8 ± 1.0	1630.1 ± 1.2	1686.0 ± 1.3
DPC, synthetic (n = 2)	24	8.0 ± 0.71	1630.4 ± 0.2	1685.2 ± 0.4
DPC, recombinant (n = 3)	24	7.8 ± 0.4	1630.1 ± 0.1	1685.4 ± 0.1
synthetic in PBS (no detergent, in reaction vials) (n = 1)	24	7.2	1623.1	1684.5
recombinant in PBS (no detergent, in reaction vials) (n = 1)	24	8.7	1621.7	1684.3
synthetic in PB in CaF_2 cuvette, pD 7.4 at 0 °C (n = 3)	0.5	12.9 ± 0.2	1626.8 ± 0.4	1682.9 ± 0.8
synthetic in PB in CaF_2 cuvette, pD 7.4 at 37 °C (n = 3)	10	9.2 ± 0.1	1624.1 ± 0.6	1685.6 ± 0.5
recombinant in PB in CaF_2 cuvette, pD 7.4 at 0 °C (n = 3)	0.5	12.9 ± 0.4	1625.7 ± 0.5	1682.8 ± 0.2
recombinant in PB in CaF_2 cuvette, pD 7.4 at 37 °C (n = 3)	10	9.1 ± 0.2	1623.0 ± 0.8	1685.2 ± 0.45
synthetic in PB in CaF_2 cuvette, pD 8.5 at 0 °C (n = 1)	0.5	14.1	1627.5	n.d.
synthetic in PB in CaF_2 cuvette, pD 8.5 at 37 °C (n = 1)	10	10.6	1624.2	1685.2
recombinant in PB in CaF_2 cuvette, pD 8.5 at 0 °C (n = 2)	0.5	17.4 ± 0.4	1628.4 ± 0.4	n.d.
recombinant in PB in CaF_2 cuvette, pD 8.5 at 37 °C (n = 2)	10	11.3 ± 0.4	1623.1 ± 0.1	1685.1 ± 0.0

[a]PB = phosphate buffer; n.d. = not detected.

considerations.[52−54] Furthermore, a combined experimental−computational study of mixtures of unlabeled and ^{13}C-labeled peptides concluded that each peptide molecule contributes at least two adjacent β-strands to the β-sheets of the oligomers, which is consistent with an antiparallel β-hairpin structure.[55] Other biophysical techniques have also indicated an at least partially antiparallel orientation of the β-strands in Aβ oligomers.[56−62] The β-sheet conformation of oligomers in this study was also confirmed by their far-ultraviolet circular dichroism (far-UV CD) spectra (Figure 8), where a maximum at 195 nm and a minimum at 215−220 nm is detected, which is typical for β-sheets.[63]

The absorbance spectra of these samples, shown in Figure 7B, reveal interesting differences between the SDS- and the DPC-stabilized oligomers. The high wavenumber band of β-sheets is relatively reduced in the spectrum of the DPC-stabilized oligomers, which is in line with less antiparallel β-sheet structure in DPC-stabilized oligomers. This property can also be seen in the second derivative spectra (Figure 7A), where the high wavenumber band is less intense for DPC-stabilized oligomers than for SDS-stabilized oligomers. It is also reflected in the β-sheet organizational index,[64] which appears to be lower for the DPC-stabilized oligomers from both sources than for the SDS-stabilized oligomers (Table 2). This index is between 0.2 and 0.3 for proteins with antiparallel β-sheets including Aβ oligomers, but below 0.06 for a parallel β-sheet protein and Aβ and α-synuclein fibrils.[64] The values for the SDS-stabilized oligomers indicate a structure rich in antiparallel β-sheets, in particular for the globulomers, whereas those for the DPC-stabilized oligomers suggest a mixed orientation of the strands in the β-sheets.

Table 2. β-Sheet Organizational Index for Aβ42 Oligomer Preparations[a]

Aβ42 oligomer	β-sheet organizational index
0.05% SDS, synthetic (n = 4)	0.30 ± 0.06
0.05% SDS, recombinant (n = 3)	0.35 ± 0.1
0.2% SDS, synthetic (n = 3)	0.24 ± 0.02
0.2% SDS, recombinant (n = 1)	0.26
DPC, synthetic (n = 2)	0.16 ± 0.04
DPC, recombinant (n = 3)	0.21 ± 0.04
synthetic in PB in CaF_2 cuvette, pD 7.4 at 20 °C (t = 1.5 h) (n = 2)	0.21 ± 0.00
synthetic in PB in CaF_2 cuvette, pD 7.4 at 37 °C (t = 2.5−3.5 h)[b] (n = 2)	0.26 ± 0.01
synthetic in PB in CaF_2 cuvette, pD 7.4 at 37 °C (t = 7.5 h) (n = 2)	0.32 ± 0.01
synthetic in PB in CaF_2 cuvette, pD 7.4 at 37 °C (t = 16.5or 17.5 h) (n = 2)	0.31 ± 0.00
recombinant in PB in CaF_2 cuvette, pD 7.4 at 20 °C (t = 1.5 h) (n = 2)	0.20 ± 0.05
recombinant in PB in CaF_2 cuvette, pD 7.4 at 37 °C (t = 2.5−3.5 h)[b] (n = 2)	0.27 ± 0.01
recombinant in PB in CaF_2 cuvette, pD 7.4 at 37 °C (t = 7.5 h) (n = 2)	0.32 ± 0.05
recombinant in PB in CaF_2 cuvette, pD 7.4 at 37 °C (t = 17.5 h) (n = 2)	0.3 ± 0.01

[a]PB = phosphate buffer. [b]The values for the first three time points at 37 °C were averaged.

The absorption around 1650 cm^{-1} is stronger for the SDS-stabilized oligomers, which indicates a higher content of non-β-sheet secondary structures in SDS-stabilized oligomers than

https://dx.doi.org/10.1021/acschemneuro.0c00642
ACS Chem. Neurosci. 2021, 12, 473−488

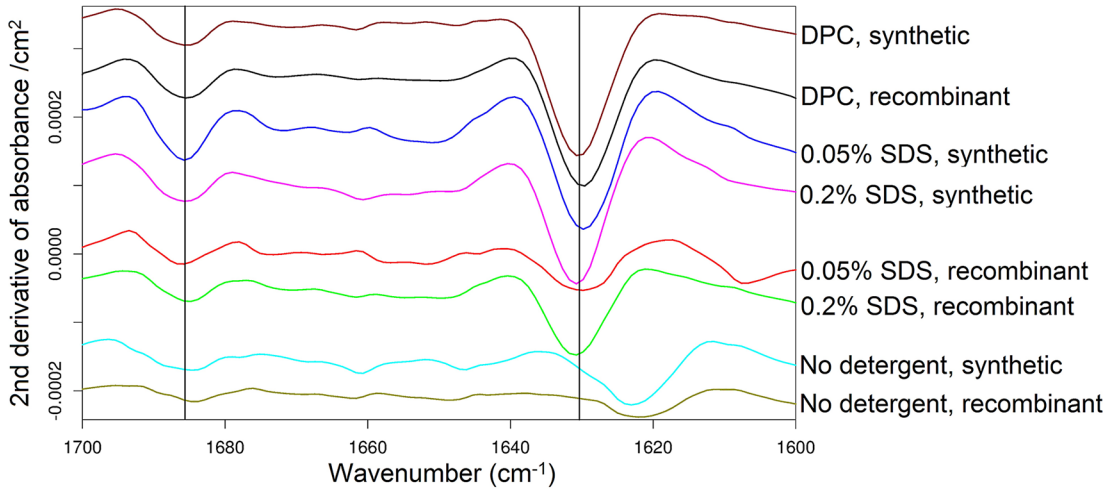

Figure 9. Second derivatives of IR absorbance spectra of synthetic and recombinant Aβ42 oligomers after 24 h of incubation in low-binding reaction tubes under different conditions. The purpose of the vertical lines is to guide the eye. Spectra are shown for individual experiments.

in DPC-stabilized oligomers. On the other hand, the β-sheet band near 1630 cm^{-1} seems to be broader for DPC-stabilized oligomers with absorption on both sides of the main band, suggesting several β-sheet bands and therefore a larger variety of β-sheet structures for DPC-oligomers. This is in line with the assumption of a mixture of parallel and antiparallel β-sheets. These additional β-sheet bands are also present, but less obviously so, in the second derivative spectrum of Figure 7A, where expected positive intensity on both sides of the negative main band is missing in the spectrum of the DPC-stabilized oligomers. Positive intensity on both sides of the main minimum is an intrinsic property of second derivative spectra. The absence of the expected positive intensity can be explained by superimposed negative intensity from absorption bands on both sides of the main band in the second derivative spectrum of DPC-stabilized oligomers. In contrast, the expected positive intensity is seen on both sides of the negative main band for the SDS-stabilized oligomers, which indicates a more uniform β-sheet structure of these oligomers.

Correlation between FTIR Spectrum and Aβ42 Oligomer Size. A general comparison of the second derivative spectra for the different Aβ42 oligomers prepared in this study is presented in Figure 9 and Table 1. A notable difference between the spectra for oligomers formed in the presence and absence of detergents (SDS or DPC) is the wavenumber at which the main, low wavenumber β-sheet band is observed. It varies from 1630 cm^{-1} in case of detergent-stabilized oligomers to 1622 cm^{-1} for heterogeneous oligomer populations and suggests that a relationship is found between the position of the main band and the size of the oligomeric assemblies: The smallest oligomers including 0.2% SDS-stabilized and DPC-stabilized oligomers exhibit the main band at 1630.1−1630.4 cm^{-1}, while globulomers (0.05% SDS-stabilized oligomers) produce the main band at 1629.1−1629.6 cm^{-1}. A similar band shift between smaller and larger SDS-stabilized oligomers has also been observed in a preliminary report of this study using a simpler preparation for the monomeric peptide.[65] The band position of the globulomer preparation shifts to lower wavenumber with time (1626.8 cm^{-1} after 5 days), due to a slow formation of larger oligomers as observed previously with gel electrophoresis.[19] Oligomeric solutions prepared in the absence of any detergents are heterogeneous mixtures, which contain larger structures (Figure 6, lanes 2 and 3) and generate the main band at much lower wavenumbers, around 1621.9−1622.9 cm^{-1}. The high wavenumber band of antiparallel β-sheets proved less variable and thus less useful for a size-spectrum correlation. Its position is only 1−2 cm^{-1} higher for nondetergent-containing oligomers as compared to detergent-stabilized oligomers.

These results are consistent with spectrum calculations, which predict a downshift of the main β-sheet band upon increasing the number of strands[52,54,66] and with an empirical correlation.[48] The sensitivity of the IR spectrum is strongest when the number of strands is small and levels off for more than approximately 10 strands for flat β-sheets.[52] The band position is also affected by the twist of β-sheets, with a more planar sheet producing a lower wavenumber of the main β-sheet band.[48,54,67] Thus, it can be presumed that the wavenumber-size correlation extends beyond 10 strands, when a larger size implies a more planar sheet as in the case of β-barrels.

Because we prepared our Aβ42 samples in D_2O-based buffers, our band positions cannot readily be compared to other reports where oligomers were prepared in H_2O-based buffers and studied in the dry state. This is because, in deuterated medium, the replacement of acidic hydrogen atoms with deuterium leads to a downshift of amide I bands (then termed amide I′ bands). Compared to other studies of Aβ40 and Aβ42 aggregates in D_2O,[27,68−71] the wavenumber of the main β-sheet band of our detergent-stabilized Aβ42 oligomers is several inverse centimeters (cm^{-1}) higher. This is in line with the small size of the detergent-stabilized oligomers and the correlation between oligomer size and band position of the main β-sheet band established in this work: Lower main band wavenumbers in the IR spectra are associated with larger oligomeric assemblies. When Aβ42 is left to aggregate in the absence of detergent, the band position is within the range of the previous studies.

In this context, it is relevant to discuss an ATR-FTIR study by Bisceglia et al. on Aβ42 oligomers of different sizes.[72] They prepared Aβ42 oligomers by aging in different buffers at neutral pH without detergents and used ultrafiltration for size discrimination. Oligomers smaller than 50 kDa exhibited their main band in the amide I region at higher wavenumber than larger oligomers. This is in agreement with the size−spectrum correlation established in our study.

https://dx.doi.org/10.1021/acschemneuro.0c00642
ACS Chem. Neurosci. 2021, 12, 473−488

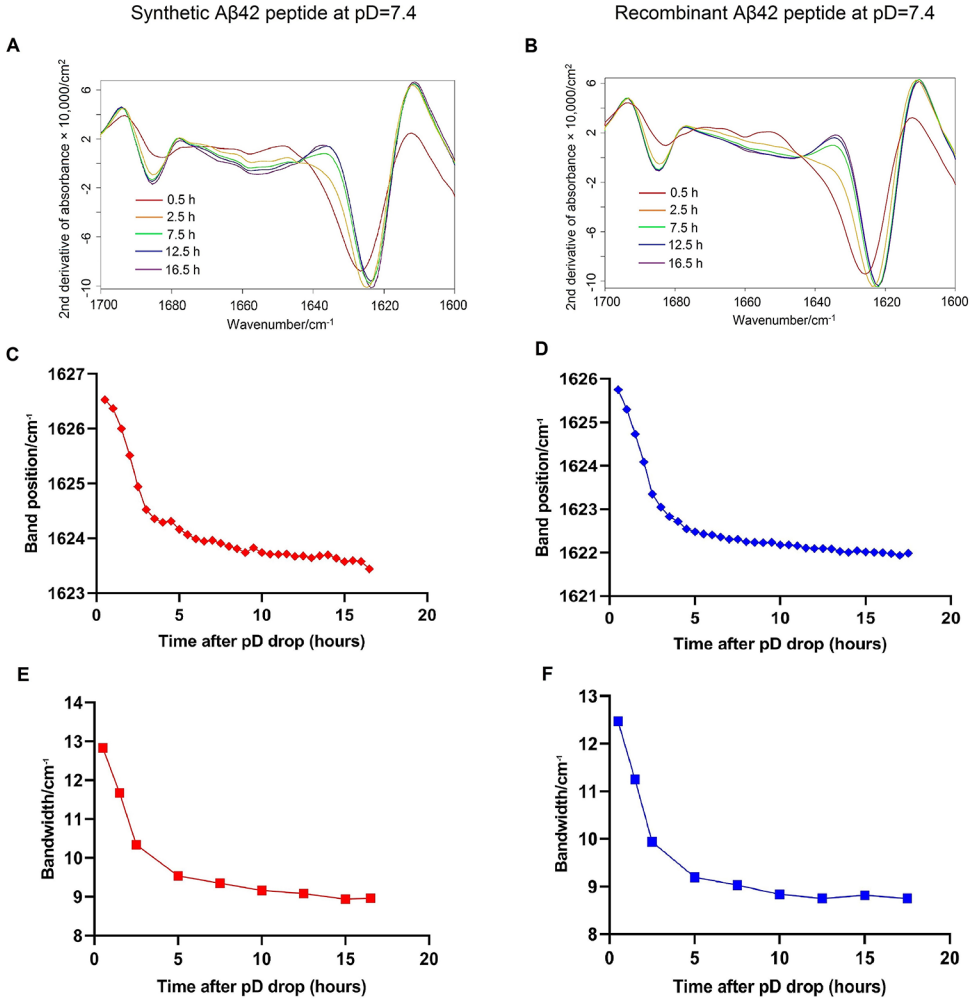

Figure 10. IR spectroscopy of aggregating synthetic (A, C, E) and recombinant (B, D, F) Aβ42 peptide at pD 7.4 inside IR cuvettes. The spectra and the spectral parameters are shown for a typical experiment for each peptide. (A, B) Second derivatives of IR absorbance spectra. The red spectrum was recorded after 30 min and at 0 °C. The other spectra were recorded at 37 °C. (C, D) Band position and (E, F) bandwidth of the main band in the amide I′ region during aggregation.

Another interesting parameter is the bandwidth in the IR spectra, which reflects the structural variety of the molecules in the sample.[28,73] Accordingly, a wide β-sheet band indicates a mixture of β-sheet structures with different sizes and twists. A narrow band, on the other hand, is evidence for a more homogeneous structure of the β-sheets in the sample. The bandwidth of our detergent-stabilized oligomers is 8 cm^{-1} or less in the second derivative (Table 1) corresponding to a bandwidth at half height in the absorbance spectra of about 10 cm^{-1}. Such a narrow bandwidth indicates well-structured β-sheets with very similar sizes and twists, which agrees with the single bands observed on BN-PAGE gels (Figures 1 and 2).

The width is narrower in most cases (Table 1) for detergent-stabilized oligomers than for oligomers prepared without detergent. This difference is most pronounced when detergent-free samples shortly after initiation of aggregation are compared to detergent-stabilized oligomers, which reflects the importance of detergents to prepare homogeneous oligomers of defined small size.

The bandwidths for synthetic SDS-stabilized Aβ42 oligomers are smaller than those for the recombinant peptide in the same oligomeric state (Table 1). This indicates more homogeneous oligomer populations for synthetic Aβ42, which is in agreement with the BN-PAGE results (Figure 1), where synthetic Aβ42 produces sharper and more intense bands than the recombinant peptide. Other IR spectroscopic features of Aβ42 oligomers from synthetic and recombinant sources are very similar, especially the band position.

Time-Resolved FTIR Studies of Aβ42 Oligomerization. With the knowledge of the oligomer size−wavenumber relationship, we performed time-resolved experiments of Aβ42 aggregation. In these experiments, the solution of the monomeric peptide at alkaline pD was mixed with dried phosphate buffer (pD values of either 7.4 or 8.5) on a flat IR spectroscopy CaF_2 window. This led to a rapid decrease in the pD of the peptide solution from above 12 to that of the buffer used. The pD drop triggered the aggregation of the peptide, as detected by transmission IR spectroscopy. The measurements started 20−30 min after mixing and assembling the IR cuvette. To capture the early intermediates in the aggregation process, the spectra were initially recorded at 0 °C, followed by two measurements at 20 °C and about 30 measurements at 37 °C. The signals were measured in 30 min intervals. At the end of the kinetic experiment, a CD spectrum was recorded for the pD 7.4 sample and is shown in Figure 8. The IR results for pD

https://dx.doi.org/10.1021/acschemneuro.0c00642
ACS Chem. Neurosci. 2021, 12, 473−488

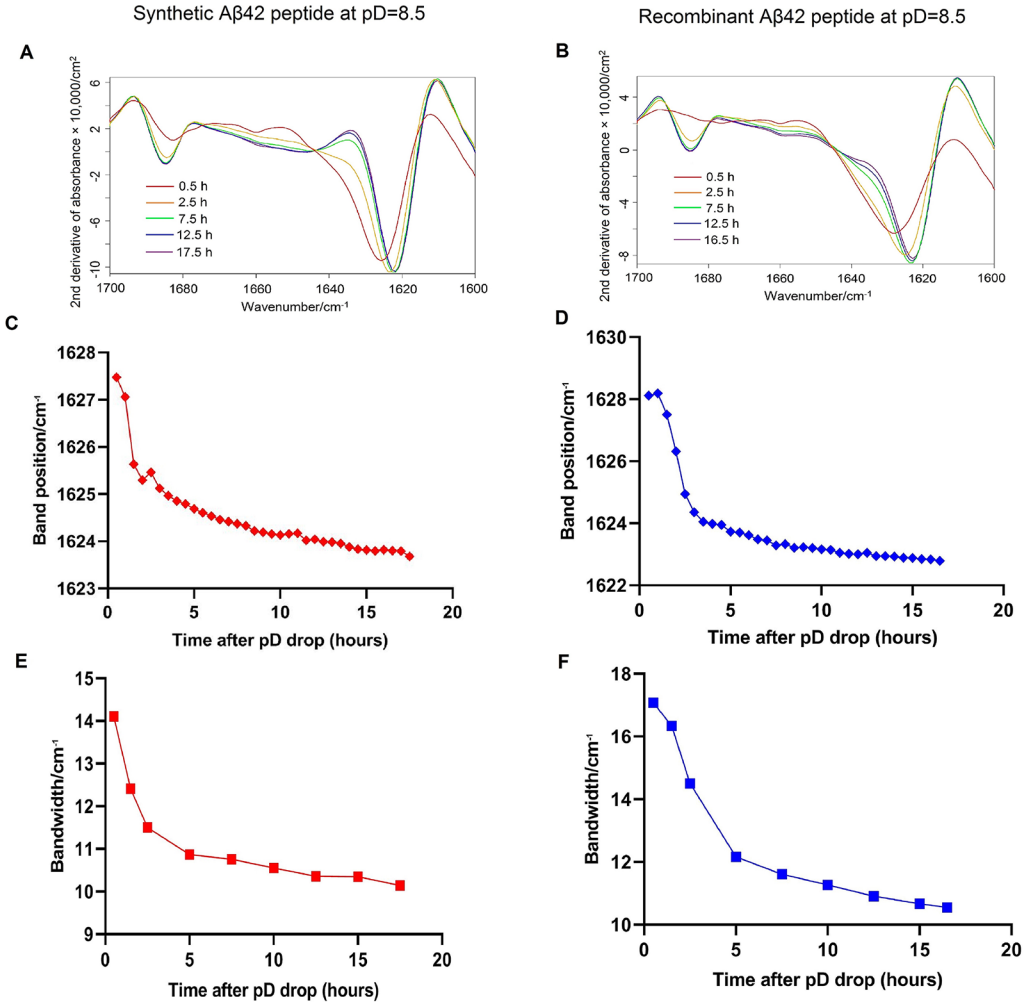

Figure 11. IR spectroscopy of aggregating synthetic (A, C, E) and recombinant (B, D, F) Aβ42 peptide at pD 8.5 inside IR cuvettes. The spectra and the spectral parameters are shown for a typical experiment for each peptide. (A, B) Second derivatives of IR absorbance spectra. The red spectrum was recorded after 30 min and at 0 °C. The other spectra were recorded at 37 °C. (C, D) Band position and (E, F) bandwidth of the main band in the amide I′ region during aggregation.

7.4 are shown in Figure 10 and Figure S1 of Supporting Information (SI), and those for pD 8.5 are shown in Figure 11.

The overall shape of the absorbance spectra in Figure S1 resembles initially that of the DPC-stabilized oligomers with little absorbance in the central region of the amide I band but later becomes similar to that of the SDS-stabilized oligomers due to an increased absorption around 1650 cm^{-1}. The high wavenumber band behaves accordingly; it is initially relatively small, and the β-sheet organizational index is low but increases within the first hours of the experiment, which is reflected in a larger index (Table 2). The range between ~0.2 and ~0.3 is in line with previous work on Aβ oligomers by us[71] and others.[64] There is no significant decrease of the β-sheet organizational index toward the end of the kinetic experiment, which indicates that there is no or only little fibril formation.

Despite similarities in spectral shape, the band positions are different for detergent-stabilized oligomers and the oligomers in the time-resolved experiment. This is seen in the second derivative spectra, which are displayed in panels A and B of Figures 10 and 11. As evident for both the synthetic and the recombinant Aβ42 peptide, the first IR spectrum (taken 20−30 min after the pD drop at 0 °C) exhibits a characteristic main band around 1626 cm^{-1} (pD 7.4) or 1628 cm^{-1} (pD 8.5). In addition, a high wavenumber band appears at about 1682−1683 cm^{-1} (pD 7.4). These features resemble those of the detergent-stabilized oligomers, but the position of both bands is lower at the beginning of the kinetic experiment. Over time and with an increase in temperature, the two bands shift in reverse directions: A downshift for the main, low wavenumber band and an upshift for the small, high wavenumber band are observed. The changes in position of the main band over time are depicted in panels C and D of Figures 10 and 11. The main band shifts considerably when the temperature is increased and further during the first hours of incubation at 37 °C; however, the pace of the shift slows down after 4 h. IR spectra at pD 7.4 recorded almost 1 week after start of the experiment and incubation of the sample at 37 °C appear almost unchanged compared to the last spectrum in the time series (downshift $\leq$ 0.2 cm^{-1}). Therefore, the position of the main band is stabilized after almost 18 h from the start of the experiment. Corresponding band shifts have been observed previously for Aβ40[74,75] and Aβ42[65,76,77] but, except for our preliminary work,[65] were only once related to oligomer size.[75]

In comparison with pD 7.4, the main IR band at pD 8.5 is found at a higher wavenumber throughout most of the time-resolved experiments, indicating smaller aggregates at pD 8.5

https://dx.doi.org/10.1021/acschemneuro.0c00642
ACS Chem. Neurosci. 2021, 12, 473−488

than pD 7.4 particularly at the start and at the end of the experiment. Recombinant and synthetic peptides behave similarly, but the recombinant peptide tends to have a lower wavenumber at a given time of the experiment.

The changes in the second derivative spectrum that lead to the discussed band shift are not symmetrical on both sides of the minimum. The shift is mostly due to the disappearance of negative intensity on the high wavenumber side of the minimum, caused by the disappearance of smaller size oligomers. It is to a lesser extent due to developing negative intensity on the low wavenumber side, resulting from the formation of larger structures. These asymmetric changes make the band narrower with time as shown in panels E and F of Figures 10 and 11 and collected in Table 3. This effect has been noted before.[74,75]

Table 3. Bandwidth at Half-Height for the Main Band in Second Derivative Spectra of the Amide I′ Region[a]

	bandwidth (in cm^{-1}) for synthetic Aβ42		bandwidth (in cm^{-1}) for recombinant Aβ42	
time point (h)	pD 7.4 (n = 2)	pD 8.5 (n = 1)	pD 7.4 (n = 2)	pD 8.5 (n = 2)
0.5	12.9 ± 0.2	14.1	13.8 ± 0.6	17.4 ± 0.4
1.5	11.6 ± 0.0	12.4	12.2 ± 0.8	16.0 ± 0.4
2.5	10.3 ± 0.1	11.5	10.8 ± 0.4	14.5 ± 0.0
5	9.5 ± 0.1	10.9	9.8 ± 0.0	12.3 ± 0.2
7.5	9.3 ± 0.1	10.8	9.3 ± 0.2	11.7 ± 0.1
10	9.2 ± 0.0	10.6	9.1 ± 0.1	11.3 ± 0.4
12.5	9.0 ± 0.1	10.4	8.9 ± 0.1	11 ± 0.1
15	8.9 ± 0.0	10.3	8.8 ± 0.0	10.7 ± 0.1

[a]During the aggregation of synthetic and recombinant Aβ42 in IR cuvettes (n = number of experiments).

Most of the bandwidth change occurs in the first 5 h, and it stabilizes after about 10 h. Similar effects are observed for peptides from the two sources, but the bandwidth is larger for the recombinant peptide at any time point (Table 3). The band is wider at pD 8.5 than at pD 7.4, which is particularly notable for the recombinant Aβ42 peptide during the first 5 h. According to these observations, the β-sheet population produces more heterogeneous IR spectra at the beginning of the experiment than at its end, at pD 8.5 than at pD 7.4, and with recombinant rather than with synthetic peptide. As the IR spectrum is most sensitive to changes in the number of β-strands when this number is small (see previous section), we expect the bandwidth to reflect mostly the concentration of small oligomers. Supporting this interpretation, the spectral changes are found on the "small oligomer side" of the β-sheet band as discussed above. Also, SDS-PAGE results (Figure 5) indicate that the low molecular weight species (monomers, trimers, and tetramers) are readily observed after 30 min from the pD drop (particularly for the synthetic peptide), while they are less abundant at pD 8.5 and mostly consumed at pD 7.4 after about 18 h, at which time the spectroscopic signals have stabilized.

The far-UV CD spectrum for the oligomeric solution of synthetic Aβ42 formed after about 18 h of incubation at 37 °C during the time-resolved aggregation experiment (Figure 8) shows a maximum band at 195−200 nm and a minimum at 215−220 nm, which confirms the β-sheet conformation of the aggregates.[63]

In summary, the combined results from the SDS-PAGE and IR spectroscopy indicate an increase in oligomer size during the first hours of the aggregation experiment, which is associated with the consumption of smaller aggregates. This results in a more homogeneous IR absorption of the β-sheets of the different aggregates. After 5 h, the signals change very little.

CONCLUSIONS

Our study adds two spectroscopic markers to the tool box of amyloid researchers: the spectral position and bandwidth of the main amide I band of β-sheets. The band position correlates with oligomer size/molecular weight, because it depends on the twist and strand number of β-sheets, particularly when the sheets are small. Hence, oligomers of different sizes prepared in this study exhibited different band positions. In kinetic aggregation experiments, the main band shifts toward lower wavenumbers, as oligomers grow in size and their β-sheet structures become more extended and/or more flat. As the correlation was established for oligomers during the first hours of aggregation, it may not apply to later aggregates and to fibrils. Fibril formation has been shown to shift the amide I band up,[75,77] but not always.[74] An upshift upon formation of the parallel β-sheets of fibrils is expected from spectrum calculations[53,54] and can be explained by different vibrational coupling in parallel β-sheets as compared to antiparallel β-sheets. An upshift is further anticipated upon fibril formation, because this leads to the stacking of β-sheets.[78]

As a consequence of the correlation, the IR bandwidth reflects the heterogeneity of the ensemble of β-sheet structures in the sample, with narrower IR bands indicating less heterogeneity. Accordingly, we found the β-sheet structures to be more homogeneous in Aβ42 oligomers in the presence of detergent than in its absence, in SDS-stabilized oligomers with the synthetic peptide than in those with the recombinant peptide, and after several hours of aggregation than at its beginning. The small width of the main negative β-sheet band in the second derivative spectra and the clear presence of positive intensity on both sides of it testify the homogeneity of the SDS-stabilized oligomers: These spectral features are particularly remarkable as the spectrum is most sensitive to oligomer size in this low molecular weight range. Additionally, they demonstrate a well-defined β-sheet structure, which is also supported by the high β-sheet organizational index of these preparations. These oligomers are therefore well-suited for further structural studies, in particular the SDS-stabilized oligomers from the synthetic peptide. The narrow band of the SDS-stabilized oligomers is in remarkable contrast to the wide bands in the absence of detergents observed early in the aggregation process. In contrast to the SDS-stabilized oligomers, those stabilized by DPC seem to be less homogeneous, as the spectrum contains additional β-sheet bands and the β-sheet organizational index suggests a mixture of parallel and antiparallel β-sheets.

We conclude that the IR spectrum can be used not only to analyze the secondary structure of the aggregates but also their size and their size distribution. These observations will be useful for the continued study of the structures and dynamics of prefibrillar assemblies of amyloidogenic peptides and proteins in general.

https://dx.doi.org/10.1021/acschemneuro.0c00642
ACS Chem. Neurosci. 2021, 12, 473−488

METHODS

Preparation of Monomeric Aβ42 Peptide Solutions. Synthetic, hexafluoroisopropanol (HFIP) treated Aβ42 (JPT Peptide Technologies, Germany) and recombinant, ultrapure, NH_4OH treated Aβ42 (rPeptide, USA) were bought as vials of 1 mg of lyophilized powder. In order to prepare aggregate free, monomeric solutions of Aβ42, the method developed by Broersen et al.[79] was used with some modifications. For both, synthetic and recombinant peptide, 1 mg of lyophilized peptide powder was dissolved in 250 μL of dimethyl sulfoxide (DMSO) to obtain a peptide concentration of 4 mg/mL. A HiTrap Desalting column (GE Healthcare, USA) was used to separate monomeric peptide from aggregates and from low molecular weight compounds in the purchased peptide samples. The column was equilibrated with 25 mL of 5 or 10 mM NaOH and 50 mM NaCl (pH 12.0−12.3) in H_2O, followed by washing with about 10−15 mL of the elution buffer: 5 or 10 mM NaOD and 50 mM NaCl in D_2O (pD 12.4−12.7). pD values were calculated by adding 0.4 units to the pH-meter reading.[80] The FTIR spectrum of the D_2O-based eluent from the column was recorded and monitored to ensure that it was H_2O-free. The peptide solution in DMSO was applied to the column, followed by pumping of 1.25 mL of the elution buffer prior to collection of peptide-containing fractions. At a flow rate of 1 mL/min, 10 peptide-containing fractions of 100−120 μL volumes were collected on ice. The peptide concentration of each eluted fraction was determined by measuring the UV absorbance at 280 nm using a NanoDrop instrument (Eppendorf, Germany), with the Aβ42 molar extinction coefficient of 1280 M^{-1} cm^{-1}.[81] Collected fractions (100−120 μL) were flash frozen in liquid nitrogen, topped with argon gas, and stored at −80 °C until they were used. Low-binding tubes were used for preparation and storage of monomers and oligomers of Aβ42.

An important modification with respect to the original protocol[79] is our use of D_2O-based buffers in order to study our Aβ42 samples with transmission FTIR spectroscopy. Using D_2O as the solvent helps to avoid the interfering strong band from the bending vibration of H_2O, which otherwise covers the region of interest (amide I region) in IR studies of proteins.

Preparation of Homogeneous Aβ42 Oligomers. Homogeneous Aβ42 oligomers were prepared according to protocols developed by Barghorn et al.[19] and Serra-Batiste et al.[22] with some modifications. SDS (Sigma, USA) was used at concentrations of 0.05 and 0.2% to induce formation of two different sizes of Aβ42 oligomers. Solutions of 5X concentrated PBS buffer in D_2O (100 mM NaH_2PO_4, 700 mM NaCl, pD 6.25) were prepared. After pD adjustment, SDS was added to 5X buffers at concentrations of either 1 or 0.25%. These 5X SDS-containing buffer solutions were mixed with 100−120 μM monomeric peptide solution, pD 12.7 (1 volume of 5X concentrated PBS buffer with 4 volumes of the peptide in the alkaline elution solution), to obtain solutions of 80−100 μM of Aβ42 peptide in PBS (20 mM NaH_2PO_4, 140 mM NaCl, pD 7.4). The pD value of the peptide solution was estimated from a separate experiment where larger volumes of buffer and peptide-free NaOD solution (pD 12.4−12.7) were mixed to measure the pD. The final SDS concentration was either 6.9 mM (0.2%) or 1.7 mM (0.05%).

In parallel experiments, DPC (Merck, Germany) was used to induce oligomer formation. Concentrated buffer (5X) in D_2O (50 mM Tris-HCl, pD 8.5) was prepared and mixed with 4 volumes of 100−120 μM monomeric peptide solution (pD 12.4−12.7) to obtain solutions of 80−100 μM Aβ42 in 10 mM Tris-HCl, pD 9. The DPC concentration in the 5X buffer (19−27 mM) was chosen so that after mixing, the ratio of the molar concentrations of Aβ42 and DPC micelles was about 2:1, according to the original protocol.[22]

The above-described mixtures of peptides and detergents were incubated at 37 °C (no shaking) for 24 h, flash frozen in liquid nitrogen, and stored at −20 °C. For each oligomer, the same preparation was used for gel electrophoresis, IR spectroscopy, and CD spectroscopy.

Preparation of Heterogeneous Aβ42 Oligomer Solutions. In addition to the detergent-stabilized oligomer preparations, peptide samples were mixed with D_2O-based PBS buffer as described above for the SDS-stabilized oligomers, but without detergent and incubated for 24 h at an Aβ42 concentration of 80−100 μM. These preparations were used for gel electrophoresis and FTIR spectroscopy. They proved to have a heterogeneous oligomer population. Alternatively, heterogeneous oligomer samples were prepared for time-resolved FTIR studies as described in the respective section below.

BN-PAGE and SDS-PAGE Analysis. Our Aβ42 samples were analyzed with both native and denaturing gel electrophoresis. BN-PAGE was conducted using 4−16% Bis-Tris Novex gels (ThermoFisher Scientific, USA) and the Invitrogen native PAGE system (ThermoFisher Scientific, USA), according to the instructions. The Amersham High Molecular Weight Calibration Kit for native electrophoresis (GE Healthcare, USA) was used as the protein marker. SDS-PAGE analysis was performed with two types of gels and buffer systems: Tris-glycine or Laemmli and Tris-Tricine (Bio-Rad, USA). Either Mini-PROTEAN TGX Precast Gels (Bio-Rad, U.S) or 16.5% Mini-PROTEAN Tris-Tricine Gels (Bio-Rad, USA) were used together with the corresponding buffers and the electrophoresis apparatus (Bio-Rad, USA). Precision Plus Protein Dual Color Standard (Bio-Rad, USA) was loaded alongside the samples for size estimation. Electrophoresis was conducted according to the instructions from Bio-Rad. Samples were not heated prior to SDS-PAGE analysis, in order to avoid degradation of the Aβ42 oligomers. Both native and SDS-PAGE gels were silver stained using the Pierce Silver Stain kit (ThermoFisher Scientific, USA), according to the instructions.

The molecular weight of the oligomers of the gel in Figure 1 was evaluated in the following way: Two gels containing the standard marker proteins and a monomeric sample were aligned with the marker proteins of the gel in Figure 1. The bands of the three marker proteins with the lowest molecular weights and the monomer band were used to generate two calibrations curves that related the locations of either the upper or the lower band limit to the molecular weight. The calibration curves were then used to estimate the molecular weight of the oligomers from the upper and lower limits of their bands.

Western Blot Assay. SDS-PAGE separated oligomeric solutions on Tris-glycine gels were transferred to PolyVinylidene DiFluoride (PVDF) membranes (Immobilon-P Millipore, USA) with the traditional wet transfer method.[82] PVDF membranes were activated in methanol for 2 min and washed with the transfer buffer (Tris buffered saline with 0.1% Tween-20, TBST) for 10 min. A transfer stack was prepared with the Tris-glycine gel and the activated membrane. Wet transfer was performed overnight at a constant current of 10 mA at 4 °C. The membrane was blocked in 5% nonfat dry milk powder (ITW reagents, Germany) in TBST for 1 h at room temperature. The membrane was incubated overnight in a 1:1000 solution of mouse monoclonal anti-Aβ antibody 6E10 (BioLegend, USA) in the blocking solution at 4 °C. After excessive washing with TBST, the membrane was incubated in 1:5000 solution of horseradish peroxidase conjugated secondary antibody (donkey antimouse IgG (H + L) antibody, ThermoFisher Scientific, USA) in the blocking solution for 1 h at room temperature. The membrane was washed thoroughly in TBST, and the protein bands were developed with WesternBright ECL substrate solution (Advansta, USA) according to the instructions.

FTIR Spectroscopy of Monomeric and Detergent-Stabilized Aβ42. Transmission IR spectra were recorded on a Tensor 37 FTIR spectrometer (Bruker Optics, Germany), continuously purged with CO_2-free dry air and equipped with an HgCdTe detector cooled with liquid nitrogen. To assemble the IR cuvettes, 5−6 μL of the samples were loaded between two flat CaF_2 windows, separated by a 50 μm plastic spacer covered on outer edges with vacuum grease. The assembled cuvette was mounted into a sample shuttle making it possible to acquire both background and sample spectra without opening the sample chamber. When recording the spectra for Aβ monomer solutions, the instrument's cuvette holder was cooled down to 0 °C with the assistance of an external water bath. Otherwise, all spectra were recorded at room temperature. A time period of about

https://dx.doi.org/10.1021/acschemneuro.0c00642
ACS Chem. Neurosci. 2021, 12, 473−488

20 min after closing the chamber lid ensured complete purge of CO_2 and water vapor. Transmission FTIR spectra were acquired in the 1900−800 cm^{-1} range with a resolution of 2 cm^{-1} at 3 or 6 mm apertures. A germanium filter and a 25 μm cellulose membrane were used to block the light intensity above 2200 cm^{-1} and below 1500 cm^{-1}, respectively. In addition, a grid was placed in the reference position of the sample shuttle in order to reduce the light intensity of the reference beam.[83] Scans (300) were taken for each spectrum. Spectra were analyzed with OPUS 5.5 software, without subtraction of the solvent spectrum.

Time-Resolved IR Spectroscopy of Aβ42 Oligomerization. Sodium phosphate (8 μL) in D_2O buffer, either 50 mM (pD 7.4) or 200 mM (pD 8.5), was laid at the center of a flat CaF_2 window covered at the periphery with a 50 μm plastic spacer smeared with vacuum grease on both sides. The buffer was dried under vacuum to obtain a film. Subsequently, 8 μL of monomeric Aβ42 (80−100 μM in 5 mM NaOD, 50 mM NaCl solution, pD 12.4−12.7) were added and mixed with the buffer precipitate in order to lower the pD. The second window was added, the IR cuvette was assembled quickly and mounted in the sample holder of a Tensor 37 FTIR spectrometer (Bruker Optics, Germany) precooled to 0 °C. The sample holder was coupled to an external water bath to control the temperature. The OPUS software was programmed to record transmission IR spectra in 30 min intervals, starting 20−30 min after mounting the assembled IR cuvette and closing the instrument's sample chamber. The sample was incubated within the spectrometer for 1 h at 0 °C and then at 20 °C for another 1 h, followed by overnight incubation at 37 °C. Accordingly, two spectra were recorded at both 0 and 20 °C. The fifth spectrum was recorded 30 min after the temperature was raised to 37 °C, followed by repetitive measurements at 30 min intervals. Transmission IR spectra were recorded as mentioned earlier with 6 mm aperture.[83] Spectra were analyzed with OPUS 5.5 software, without subtraction of the solvent spectrum.

IR Spectra Processing. Spectra were analyzed with the OPUS 5.5 software, and second derivative spectra were calculated with a smoothing factor of 17. The width at half of the actual height of the main β-sheet band near 1630 cm^{-1} in the second derivatives was calculated and reported as the bandwidth. A solvent spectrum was not subtracted, because this changed the second derivative spectrum only marginally as shown in Figure S2 of the Supporting Information. The reason for the small impact of the solvent spectrum on the second derivative spectra is the large spectral width of the solvent bands, which leads to their suppression in second derivative spectra. For the absorbance spectra shown in Figure 7 and in Figure S1 of the Supporting Information, however, a solvent spectrum and a baseline was subtracted from the original absorbance spectrum. The baseline was generated from 6 points with 10 cm^{-1} spacing between 1750 and 1700 cm^{-1} and between 1600 and 1550 cm^{-1} which were connected by polynomes.

The β-sheet organizational index was calculated according to Celej et al.[64] from the solvent and baseline subtracted absorbance spectra. The spectra were Fourier self-deconvoluted with the Kinetics software, kindly provided by Erik Goormaghtigh (Université Libre de Bruxelles), using the same parameters as in the original publication. The deconvoluted spectra were then fitted with four component bands in the spectral range from 1700 to 1600 cm^{-1}. Then, the β-sheet organizational index was calculated by dividing the intensities of the high and low wavenumber β-sheet bands.

CD Spectroscopy. Far-UV CD spectra of the samples in the IR cuvette were acquired immediately after the IR spectra using a custom-made holder to accommodate the assembled IR cuvettes. CD spectra were recorded on a Chirascan spectrometer (Applied Photophysics, UK) in the range 185−250 nm, with a bandwidth of 2 nm at room temperature. For each measurement, 10 repeats of the spectrum were recorded and averaged.

■ ASSOCIATED CONTENT

Supporting Information

The Supporting Information is available free of charge at https://pubs.acs.org/doi/10.1021/acschemneuro.0c00642.

IR absorption spectra at different time points of the kinetic experiment with the synthetic peptide at pD 7.4 and second derivative spectra before and after the subtraction of a solvent spectrum (PDF)

■ AUTHOR INFORMATION

Corresponding Author

Andreas Barth − *Department of Biochemistry and Biophysics, Stockholm University, Stockholm SE-106 91, Sweden;* orcid.org/0000-0001-5784-7673; Phone: +46 8 162452; Email: andreas.barth@dbb.su.se

Author

Faraz Vosough − *Department of Biochemistry and Biophysics, Stockholm University, Stockholm SE-106 91, Sweden*

Complete contact information is available at: https://pubs.acs.org/10.1021/acschemneuro.0c00642

Author Contributions

A.B. designed the study. F.V. performed the experiments. A.B. and F.V. planned and evaluated the experiments and wrote the manuscript.

Funding

This work was supported by grants from the Stockholm regional council, Hjärnfonden, and Magn. Bergvalls Stiftelse. The FTIR spectrometer was funded by the Knut and Alice Wallenberg foundation.

Notes

The authors declare no competing financial interest.

■ ACKNOWLEDGMENTS

The authors are grateful to Jan Schnatwinkel for his contribution in the early phase of this project. We would also like to thank Cecilia Mörman, Sebastian K.T.S. Wärmländer, and Astrid Gräslund for assistance and advice with preparation of Aβ42 monomer solutions, and we would like to thank Grant Kemp for providing the BN-PAGE materials/apparatus. We are also grateful to Daniel Twohig for his time and help with performing of the western blot experiments and to Henrietta M. Nielsen for invaluable comments on the blot results. We thank Erik Goormaghtigh (Université Libre de Bruxelles) for generously supplying the program *Kinetics*.

■ ABBREVIATIONS

Aβ peptide, amyloid-β peptide; AD, Alzheimer's disease; ATR, attenuated total reflection; BN, blue native; DMSO, dimethyl sulfoxide; DPC, dodecyl phosphocholine; FTIR, Fourier transform infrared; HFIP, hexafluoroisopropanol; IR, infrared; PAGE, polyacrylamide gel electrophoresis; PBS, phosphate buffered saline; PVDF, PolyVinylidene DiFluoride; SDS, sodium dodecyl sulfate; TBST, Tris buffered saline with Tween 20; UV-CD, ultraviolet-circular dichroism

■ REFERENCES

(1) Wang, J., Dickson, D. W., Trojanowski, J. Q., and Lee, V. M. (1999) The levels of soluble versus insoluble brain Aβ distinguish Alzheimer's disease from normal and pathologic aging. *Exp. Neurol. 158*, 328−337.

(2) Lue, L. F., Kuo, Y. M., Roher, A. E., Brachova, L., Shen, Y., Sue, L., Beach, T., Kurth, J. H., Rydel, R. E., and Rogers, J. (1999) Soluble amyloid beta peptide concentration as a predictor of synaptic change in Alzheimer's disease. *Am. J. Pathol. 155*, 853−862.
(3) McLean, C. A., Cherny, R. A., Fraser, F. W., Fuller, S. J., Smith, M. J., Beyreuther, K., Bush, A. I., and Masters, C. L. (1999) Soluble pool of Abeta amyloid as a determinant of severity of neurodegeneration in Alzheimer's disease. *Ann. Neurol. 46*, 860−866.
(4) Mucke, L., Masliah, E., Yu, G.-Q., Mallory, M., Rockenstein, E. M., Tatsuno, G., Hu, K., Kholodenko, D., Johnson-Wood, K., and McConlogue, L. (2000) High-level neuronal expression of Aβ1−42 in wild-type human amyloid protein precursor transgenic mice: synaptotoxicity without plaque formation. *J. Neurosci. 20*, 4050−4058.
(5) Kirkitadze, M. D., Bitan, G., and Teplow, D. B. (2002) Paradigm shifts in Alzheimer's disease and other neurodegenerative disorders: The emerging role of oligomeric assemblies. *J. Neurosci. Res. 69*, 567−577.
(6) Podlisny, M. B., Ostaszewski, B. L., Squazzo, S. L., Koo, E. H., Rydell, R. E., Teplow, D. B., and Selkoe, D. J. (1995) Aggregation of secreted amyloid β-protein into sodium dodecyl sulfate-stable oligomers in cell culture. *J. Biol. Chem. 270*, 9564−9570.
(7) Harper, J. D., Wong, S. S., Lieber, C. M., and Lansbury, P. T. (1997) Observation of metastable Aβ amyloid protofibrils by atomic force microscopy. *Chem. Biol. 4*, 119−125.
(8) Walsh, D. M., Lomakin, A., Benedek, G. B., Condron, M. M., and Teplow, D. B. (1997) Amyloid β-protein fibrillogenesis. Detection of a protofibrillar intermediate. *J. Biol. Chem. 272*, 22364−22372.
(9) Lambert, M. P., Barlow, A. K., Chromy, B. A., Edwards, C., Freed, R., Liosatos, M., Morgan, T. E., Rozovsky, I., Trommer, B., Viola, K. L., Wals, P., Zhang, C., Finch, C. E., Krafft, G. A., and Klein, W. L. (1998) Diffusible, nonfibrillar ligands derived from Aβ1−42 are potent central nervous system neurotoxins. *Proc. Natl. Acad. Sci. U. S. A. 95*, 6448−6453.
(10) Enya, M., Morishima-Kawashima, M., Yoshimura, M., Shinkai, Y., Kusui, K., Khan, K., Games, D., Schenk, D., Sugihara, S., Yamaguchi, H., and Ihara, Y. (1999) Appearance of sodium dodecyl sulfate-stable amyloid β-protein (Aβ) dimer in the cortex during aging. *Am. J. Pathol. 154*, 271−279.
(11) Funato, H., Enya, M., Yoshimura, M., Morishima-Kawashima, M., and Ihara, Y. (1999) Presence of sodium dodecyl sulfate-stable amyloid β-protein dimers in the hippocampus CA1 not exhibiting neurofibrillary tangle formation. *Am. J. Pathol. 155*, 23−28.
(12) Walsh, D. M., Hartley, D. M., Kusumoto, Y., Fezoui, Y., Condron, M. M., Lomakin, A., Benedek, G. B., Selkoe, D. J., and Teplow, D. B. (1999) Amyloid β-protein fibrillogenesis. Structure and biological activity of protofibrillar intermediates. *J. Biol. Chem. 274*, 25945−25952.
(13) Walsh, D. M., Tseng, B. P., Rydel, R. E., Podlisny, M. B., and Selkoe, D. J. (2000) The oligomerization of amyloid β-protein begins intracellularly in cells derived from human brain. *Biochemistry 39*, 10831−10839.
(14) Hoshi, M., Sato, M., Matsumoto, S., Noguchi, A., Yasutake, K., Yoshida, N., and Sato, K. (2003) Spherical aggregates of beta-amyloid (amylospheroid) show high neurotoxicity and activate tau protein kinase I/glycogen synthase kinase-3β. *Proc. Natl. Acad. Sci. U. S. A. 100*, 6370−6375.
(15) Gong, Y., Chang, L., Viola, K. L., Lacor, P. N., Lambert, M. P., Finch, C. E., Krafft, G. A., and Klein, W. L. (2003) Alzheimer's disease-affected brain: presence of oligomeric A beta ligands (ADDLs) suggests a molecular basis for reversible memory loss. *Proc. Natl. Acad. Sci. U. S. A. 100*, 10417−10422.
(16) Lesné, S., Koh, M. T., Kotilinek, L., Kayed, R., Glabe, C. G., Yang, A., Gallagher, M., and Ashe, K. H. (2006) A specific amyloid-β protein assembly in the brain impairs memory. *Nature 440*, 352−357.
(17) Lynch, M. A. (2004) Long-term potentiation and memory. *Physiol. Rev. 84*, 87−136.
(18) Cooke, S. F., and Bliss, T. V. P. (2006) Plasticity in the human central nervous system. *Brain 129*, 1659−1673.
(19) Barghorn, S., Nimmrich, V., Striebinger, A., Krantz, C., Keller, P., Janson, B., Bahr, M., Schmidt, M., Bitner, R. S., Harlan, J., Barlow, E., Ebert, U., and Hillen, H. (2005) Globular amyloid β-peptide 1−42 oligomer − a homogenous and stable neuropathological protein in Alzheimer's disease. *J. Neurochem. 95*, 834−847.
(20) Rangachari, V., Moore, B. D., Reed, D. K., Sonoda, L. K., Bridges, A. W., Conboy, E., Hartigan, D., and Rosenberry, T. L. (2007) Amyloid-β(1−42) rapidly forms protofibrils and oligomers by distinct pathways in low concentrations of sodium dodecylsulfate. *Biochemistry 46*, 12451−12462.
(21) Tew, D. J., Bottomley, S. P., Smith, D. P., Ciccotosto, G. D., Babon, J., Hinds, M. G., Masters, C. L., Cappai, R., and Barnham, K. J. (2008) Stabilization of neurotoxic soluble β-sheet rich conformations of the Alzheimer's disease amyloid-β peptide. *Biophys. J. 94*, 2752−2766.
(22) Serra-Batiste, M., Ninot-Pedrosa, M., Bayoumi, M., Gairí, M., Maglia, G., and Carulla, N. (2016) Aβ42 assembles into specific β-barrel pore-forming oligomers in membrane-mimicking environments. *Proc. Natl. Acad. Sci. U. S. A. 113*, 10866−10871.
(23) Coles, M., Bicknell, W., Watson, A. A., Fairlie, D. P., and Craik, D. J. (1998) Solution structure of amyloid β-peptide(1−40) in a water-micelle environment. Is the membrane-spanning domain where we think it is? *Biochemistry 37*, 11064−11077.
(24) Shao, H., Jao, S., Ma, K., and Zagorski, M. G. (1999) Solution structures of micelle-bound amyloid β-(1−40) and β-(1−42) peptides of Alzheimer's disease. *J. Mol. Biol. 285*, 755−773.
(25) Jarvet, J., Danielsson, J., Damberg, P., Oleszczuk, M., and Gräslund, A. (2007) Positioning of the Alzheimer Aβ(1−40) peptide in SDS micelles using NMR and paramagnetic probes. *J. Biomol. NMR 39*, 63−72.
(26) Wahlström, A., Hugonin, L., Perálvarez-Marín, A., Jarvet, J., and Gräslund, A. (2008) Secondary structure conversions of Alzheimer's Aβ(1−40) peptide induced by membrane-mimicking detergents. *FEBS J. 275*, 5117−5128.
(27) Komatsu, H., Liu, L., Murray, I. V. J., and Axelsen, P. H. (2007) A mechanistic link between oxidative stress and membrane mediated amyloidogenesis revealed by infrared spectroscopy. *Biochim. Biophys. Acta, Biomembr. 1768*, 1913−1922.
(28) Barth, A. (2007) Infrared spectroscopy of proteins. *Biochim. Biophys. Acta, Bioenerg. 1767*, 1073−1101.
(29) Sarroukh, R., Goormaghtigh, E., Ruysschaert, J.-M., and Raussens, V. (2013) ATR-FTIR: a "rejuvenated" tool to investigate amyloid proteins. *Biochim. Biophys. Acta, Biomembr. 1828*, 2328−2338.
(30) Miller, L. M., Bourassa, M. W., and Smith, R. J. (2013) FTIR spectroscopic imaging of protein aggregation in living cells. *Biochim. Biophys. Acta, Biomembr. 1828*, 2339−2346.
(31) Moran, S. D., and Zanni, M. T. (2014) How to get insight into amyloid structure and formation from infrared spectroscopy. *J. Phys. Chem. Lett. 5*, 1984−1993.
(32) Hoffner, G., André, W., Sandt, C., and Djian, P. (2014) Synchrotron-based infrared spectroscopy brings to light the structure of protein aggregates in neurodegenerative diseases. *Rev. Anal. Chem. 33*, 231−243.
(33) Yang, H., Yang, S., Kong, J., Dong, A., and Yu, S. (2015) Obtaining information about protein secondary structures in aqueous solution using Fourier transform IR spectroscopy. *Nat. Protoc. 10*, 382−396.
(34) Martial, B., Lefèvre, T., and Auger, M. (2018) Understanding amyloid fibril formation using protein fragments: structural investigations via vibrational spectroscopy and solid-state NMR. *Biophys. Rev. 10*, 1133−1149.
(35) Bitan, G., Fradinger, E. A., Spring, S. M., and Teplow, D. B. (2005) Neurotoxic protein oligomers−what you see is not always what you get. *Amyloid 12*, 88−95.
(36) Watt, A. D., Perez, K. A., Rembach, A., Sherrat, N. A., Hung, L. W., Johanssen, T., McLean, C. A., Kok, W. M., Hutton, C. A., Fodero-Tavoletti, M., Masters, C. L., Villemagne, V. L., and Barnham, K. J. (2013) Oligomers, fact or artefact? SDS-PAGE induces dimerization

of β-amyloid in human brain samples. *Acta Neuropathol. 125*, 549−564.
(37) Bitan, G. (2006) Structural study of metastable amyloidogenic protein oligomers by photo-induced cross-linking of unmodified proteins. *Methods Enzymol. 413*, 217−236.
(38) Pujol-Pina, R., Vilaprinyó-Pascual, S., Mazzucato, R., Arcella, A., Vilaseca, M., Orozco, M., and Carulla, N. (2015) SDS-PAGE analysis of Aβ oligomers is disserving research into Alzheimer's disease: appealing for ESI-IM-MS. *Sci. Rep. 5*, 14809.
(39) Chromy, B. A., Nowak, R. J., Lambert, M. P., Viola, K. L., Chang, L., Velasco, P. T., Jones, B. W., Fernandez, S. J., Lacor, P. N., Horowitz, P., Finch, C. E., Krafft, G. A., and Klein, W. L. (2003) Self-assembly of Aβ1−42 into neurotoxins. *Biochemistry 42*, 12749−12760.
(40) Upadhaya, A. R., Lungrin, I., Yamaguchi, H., Fändrich, M., and Thal, D. R. (2012) High molecular weight Aβ oligomers and protofibrils are the predominant Aβ species in the native soluble protein fraction of the AD brain. *J. Cell Mol. Med. 16*, 287−295.
(41) Eckert, A., Hauptmann, S., Scherping, I., Meinhardt, J., Rhein, V., Dröse, S., Brandt, U., Fändrich, M., Müller, W. E., and Götz, J. (2008) Oligomeric and fibrillar species of β-amyloid (Aβ42) both impair mitochondrial function in P301L tau transgenic mice. *J. Mol. Med. 86*, 1255−1267.
(42) Österlund, N., Moons, R., Ilag, L. L., Sobott, F., and Gräslund, A. (2019) Native ion mobility-mass spectrometry reveals the formation of β-barrel shaped amyloid-β hexamers in a membrane-mimicking environment. *J. Am. Chem. Soc. 141*, 10440−10450.
(43) Finder, V. H., Vodopivec, I., Nitsch, R. M., and Glockshuber, R. (2010) The recombinant amyloid-β peptide Aβ1−42 aggregates faster and is more neurotoxic than synthetic Aβ1−42. *J. Mol. Biol. 396*, 9−18.
(44) Adams, D. J., Nemkov, T. G., Mayer, J. P., Old, W. M., and Stowell, M. H. B. (2017) Identification of the primary peptide contaminant that inhibits fibrillation and toxicity in synthetic amyloid-β42. *PLoS One 12*, e0182804.
(45) Hilario, J., Kubelka, J., and Keiderling, T. A. (2003) Optical spectroscopic investigations of model β-sheet hairpins in aqueous solution. *J. Am. Chem. Soc. 125*, 7562−7574.
(46) Xu, Y., Purkayastha, P., and Gai, F. (2006) Nanosecond folding dynamics of a three-stranded β-sheet. *J. Am. Chem. Soc. 128*, 15836−15842.
(47) Scheerer, D., Chi, H., McElheny, D., Keiderling, T. A., and Hauser, K. (2018) Isotopically site-selected dynamics of a three-stranded β-sheet peptide detected with temperature-jump infrared-spectroscopy. *J. Phys. Chem. B 122*, 10445−10454.
(48) Zandomeneghi, G., Krebs, M. R. H., McCammon, M. G., and Fändrich, M. (2004) FTIR reveals structural differences between native β-sheet proteins and amyloid fibrils. *Protein Sci. 13*, 3314−3321.
(49) Cerf, E., Sarroukh, R., Tamamizu-Kato, S., Breydo, L., Derclaye, S., Dufrêne, Y. F., Narayanaswami, V., Goormaghtigh, E., Ruysschaert, J.-M., and Raussens, V. (2009) Antiparallel β-sheet: a signature structure of the oligomeric amyloid β-peptide. *Biochem. J. 421*, 415−423.
(50) Yushchenko, T., Deuerling, E., and Hauser, K. (2018) Insights into the aggregation mechanism of polyQ proteins with different glutamine repeat lengths. *Biophys. J. 114*, 1847−1857.
(51) Li, H., Lantz, R., and Du, D. (2019) Vibrational approach to the dynamics and structure of protein amyloids. *Molecules 24*, 186.
(52) Chirgadze, Y. N., and Nevskaya, N. A. (1976) Infrared spectra and resonance interaction of amide-I vibration of the antiparallel-chain pleated sheet. *Biopolymers 15*, 607−625.
(53) Chirgadze, Y. N., and Nevskaya, N. A. (1976) Infrared spectra and resonance interaction of amide-I vibration of the parallel-chain pleated sheet. *Biopolymers 15*, 627−636.
(54) Kubelka, J., and Keiderling, T. A. (2001) Differentiation of β-sheet-forming structures: Ab-initio based simulations of IR absorption and vibrational CD for model peptide and protein β-sheets. *J. Am. Chem. Soc. 123*, 12048−12058.
(55) Baronio, C. M., Baldassarre, M., and Barth, A. (2019) Insight into the internal structure of amyloid-β oligomers by isotope-edited Fourier transform infrared spectroscopy. *Phys. Chem. Chem. Phys. 21*, 8587−8597.
(56) Yu, L., Edalji, R., Harlan, J. E., Holzman, T. F., Lopez, A. P., Labkovsky, B., Hillen, H., Barghorn, S., Ebert, U., Richardson, P. L., Miesbauer, L., Solomon, L., Bartley, D., Walter, K., Johnson, R. W., Hajduk, P. J., and Olejniczak, E. T. (2009) Structural characterization of a soluble amyloid beta-peptide oligomer. *Biochemistry 48*, 1870−1877.
(57) Ahmed, M., Davis, J., Aucoin, D., Sato, T., Ahuja, S., Aimoto, S., Elliott, J. I., Van Nostrand, W. E., and Smith, S. O. (2010) Structural conversion of neurotoxic amyloid-beta(1−42) oligomers to fibrils. *Nat. Struct. Mol. Biol. 17*, 561−567.
(58) Pan, J., Han, J., Borchers, C. H., and Konermann, L. (2012) Structure and dynamics of small soluble Abeta(1−40) oligomers studied by top-down hydrogen exchange mass spectrometry. *Biochemistry 51*, 3694−3703.
(59) Gu, L., Liu, C., and Guo, Z. (2013) Structural insights into Aβ42 oligomers using site-directed spin labeling. *J. Biol. Chem. 288*, 18673−18683.
(60) Gu, L., Liu, C., Stroud, J. C., Ngo, S., Jiang, L., and Guo, Z. (2014) Antiparallel triple-strand architecture for prefibrillar Aβ42 oligomers. *J. Biol. Chem. 289*, 27300−27313.
(61) Lendel, C., Bjerring, M., Dubnovitsky, A., Kelly, R. T., Filippov, A., Antzutkin, O. N., Nielsen, N. C., and Härd, T. (2014) A hexameric peptide barrel as building block of amyloid-β protofibrils. *Angew. Chem., Int. Ed. 53*, 12756−12760.
(62) Gao, Y., Guo, C., Watzlawik, J. O., Randolph, P. S., Lee, E. J., Huang, D., Stagg, S. M., Zhou, H.-X., Rosenberry, T. L., and Paravastu, A. K. (2020) Out-of-register parallel β-sheets and antiparallel β-sheets coexist in 150-kDa oligomers formed by amyloid-β(1−42). *J. Mol. Biol. 432*, 4388−4407.
(63) Greenfield, N. J. (2006) Using circular dichroism spectra to estimate protein secondary structure. *Nat. Protoc. 1*, 2876−2890.
(64) Celej, M. S., Sarroukh, R., Goormaghtigh, E., Fidelio, G. D., Ruysschaert, J.-M., and Raussens, V. (2012) Toxic prefibrillar α-synuclein amyloid oligomers adopt a distinctive antiparallel β-sheet structure. *Biochem. J. 443*, 719−726.
(65) Schnatwinkel, J. (2016) *Structure and Dynamics of Amyloid β Oligomers*, Degree project, pp 19−32, Stockholm University, Stockholm.
(66) Kubelka, J., and Keiderling, T. A. (2001) The anomalous infrared amide I intensity distribution in ^{13}C isotopically labeled peptide β-sheets comes from extended, multiple-stranded structures. An ab initio study. *J. Am. Chem. Soc. 123*, 6142−6150.
(67) Bour, P., and Keiderling, T. A. (2004) Structure, spectra and the effects of twisting of β-sheet peptides. A density functional theory study. *J. Mol. Struct.: THEOCHEM 675*, 95−105.
(68) Koppaka, V., and Axelsen, P. H. (2000) Accelerated accumulation of amyloid β proteins on oxidatively damaged lipid membranes. *Biochemistry 39*, 10011−10016.
(69) Benseny-Cases, N., Cócera, M., and Cladera, J. (2007) Conversion of non-fibrillar beta-sheet oligomers into amyloid fibrils in Alzheimer's disease amyloid peptide aggregation. *Biochem. Biophys. Res. Commun. 361*, 916−921.
(70) Abelein, A., Jarvet, J., Barth, A., Gräslund, A., and Danielsson, J. (2016) Ionic strength modulation of the free energy landscape of $A\beta_{40}$ peptide fibril formation. *J. Am. Chem. Soc. 138*, 6893−6902.
(71) Baldassarre, M., Baronio, C. M., Morozova-Roche, L. A., and Barth, A. (2017) Amyloid β-peptides 1−40 and 1−42 form oligomers with mixed β-sheets. *Chem. Sci. 8*, 8247−8254.
(72) Bisceglia, F., Natalello, A., Serafini, M. M., Colombo, R., Verga, L., Lanni, C., and De Lorenzi, E. (2018) An integrated strategy to correlate aggregation state, structure and toxicity of Aβ1−42 oligomers. *Talanta 188*, 17−26.
(73) Wharton, C. W. (2000) Infrared spectroscopy of enzyme reaction intermediates. *Nat. Prod. Rep. 17*, 447−453.

(74) Itkin, A., Dupres, V., Dufrêne, Y. F., Bechinger, B., Ruysschaert, J.-M., and Raussens, V. (2011) Calcium ions promote formation of amyloid β-peptide (1−40) oligomers causally implicated in neuronal toxicity of Alzheimer's disease. *PLoS One 6*, e18250.
(75) Sarroukh, R., Cerf, E., Derclaye, S., Dufrêne, Y. F., Goormaghtigh, E., Ruysschaert, J.-M., and Raussens, V. (2011) Transformation of amyloid β(1−40) oligomers into fibrils is characterized by a major change in secondary structure. *Cell. Mol. Life Sci. 68*, 1429−1438.
(76) Fu, Z., Aucoin, D., Davis, J., Van Nostrand, W. E., and Smith, S. O. (2015) Mechanism of nucleated conformational conversion of Aβ42. *Biochemistry 54*, 4197−4207.
(77) Hubin, E., Deroo, S., Kaminski Schierle, G., Kaminski, C., Serpell, L., Subramaniam, V., Van Nuland, N., Broersen, K., Raussens, V., and Sarroukh, R. (2015) Two distinct β-sheet structures in Italian-mutant amyloid-beta fibrils: a potential link to different clinical phenotypes. *Cell. Mol. Life Sci. 72*, 4899−4913.
(78) Karjalainen, E.-L., Ravi, H. K., and Barth, A. (2011) Simulation of the amide I absorption of stacked β-sheets. *J. Phys. Chem. B 115*, 749−757.
(79) Broersen, K., Jonckheere, W., Rozenski, J., Vandersteen, A., Pauwels, K., Pastore, A., Rousseau, F., and Schymkowitz, J. (2011) A standardized and biocompatible preparation of aggregate-free amyloid beta peptide for biophysical and biological studies of Alzheimer's disease. *Protein Eng., Des. Sel. 24*, 743−750.
(80) Glasoe, P. K., and Long, F. A. (1960) Use of glass electrodes to measure acidities in deuterium oxide. *J. Phys. Chem. 64*, 188−190.
(81) Edelhoch, H. (1967) Spectroscopic determination of tryptophan and tyrosine in proteins. *Biochemistry 6*, 1948−1954.
(82) Mahmood, T., and Yang, P.-C. (2012) Western blot: technique, theory and trouble shooting. *N. Am. J. Med. Sci. 4*, 429−434.
(83) Baldassarre, M., and Barth, A. (2014) Pushing the detection limit of infrared spectroscopy for structural analysis of dilute protein samples. *Analyst 139*, 5393−5399.

https://dx.doi.org/10.1021/acschemneuro.0c00642
ACS Chem. Neurosci. 2021, 12, 473−488